

Inhibitory Effect of a Triterpenoid Compound, with or without Alpha Interferon, on Hepatitis C Virus Infection^{∇†}

Takako Watanabe,^{1,‡} Naoya Sakamoto,^{1,2,‡*} Mina Nakagawa,^{1,2} Sei Kakinuma,^{1,2} Yasuhiro Itsui,³ Yuki Nishimura-Sakurai,¹ Mayumi Ueyama,¹ Yusuke Funaoka,¹ Akiko Kitazume,¹ Sayuri Nitta,¹ Kei Kiyohashi,¹ Miyako Murakawa,¹ Seishin Azuma,¹ Kiichiro Tsuchiya,¹ Shinya Oooka,¹ and Mamoru Watanabe¹

Department of Gastroenterology and Hepatology¹ and Department for Hepatitis Control,² Tokyo Medical and Dental University, Tokyo, Japan, and Department of Internal Medicine, Soka Municipal Hospital, Saitama, Japan³

Received 19 December 2010/Returned for modification 11 January 2011/Accepted 14 March 2011

A lack of patient response to alpha interferon (α -IFN) plus ribavirin (RBV) treatment is a major problem in eliminating hepatitis C virus (HCV). We screened chemical libraries for compounds that enhanced cellular responses to α -IFN and identified a triterpenoid, toosendanin (TSN). Here, we studied the effects and mechanisms of action of TSN on HCV replication and its effect on α -IFN signaling. We treated HCV genotype 1b replicon-expressing cells and HCV-J6/JFH-infected cells with TSN, with or without α -IFN, and the level of HCV replication was quantified. To study the effects of TSN on α -IFN signaling, we detected components of the interferon-stimulated gene factor 3 (ISGF3), phosphorylated signal transducer and activator of transcription 1 (STAT1), and STAT2 by Western blotting analysis; expression levels of mRNA of interferon regulatory factor 9 using real-time reverse transcription-PCR (RT-PCR); and interferon-stimulated response element reporter activity and measured the expression levels of interferon-inducible genes for 2',5'-oligoadenylate synthetase, MxA, protein kinase R, and p56 using real-time RT-PCR. TSN alone specifically inhibited expression of the HCV replicon (50% effective concentration = 20.6 nM, 50% cytotoxic concentration > 3 μ M, selectivity index > 146). Pretreatment with TSN prior to α -IFN treatment was more effective in suppressing HCV replication than treatment with either drug alone. Although TSN alone did not activate the α -IFN pathway, it significantly enhanced the α -IFN-induced increase of phosphorylated STATs, interferon-stimulated response element activation, and interferon-stimulated gene expression. TSN significantly increased baseline expression of interferon regulatory factor 9, a component of interferon-stimulated gene factor 3. Antiviral effects of treatment with α -IFN can be enhanced by pretreatment with TSN. Its mechanisms of action could potentially be important to identify novel molecular targets to treat HCV infection.

Hepatitis C virus (HCV) is one of the most important pathogens causing acute and chronic hepatitis, liver cirrhosis, and hepatocellular malignancies (29). Alpha interferon (α -IFN) combined with ribavirin (RBV) is the standard treatment for HCV infection (6, 10). However, virus elimination rates are about 50% among treated patients, and therapy is often accompanied by substantial side effects (6, 44). It was recently reported that genetic polymorphisms of the *IL28B* gene, which codes for lambda IFN, are critical for predicting responses to α -IFN plus RBV therapy (8, 35, 38). Patients with minor variants of *IL28B*, who comprise ~50% of Caucasian, 25% of Asian, and ~70% of African populations, showed poor responses to α -IFN treatment. Although new specific anti-HCV drugs are under development, many of them require combined use with α -IFN and RBV (26). Taken together, current difficulties in eliminating HCV are mostly attributable to the limited treatment options and to the limited activity of α -IFN

against the virus. For this reason, the development of safe and effective agents that enhance antiviral actions against HCV has been a strong motivation in academia and industry.

To search for a new agent which enhances the effect of α -IFN, we used interferon-stimulated response element (ISRE) reporter screening. We screened a chemical library (60,500 compounds) for compounds that enhance ISRE activity when they are used in combination with α -IFN, using ISRE reporter screening, and identified several compounds that increased the ISRE reporter activities when they are used in combination with α -IFN and that did not show cytotoxicity. Among the hit compounds, toosendanin (TSN; C₃₀H₃₈O₁₁; molecular weight = 574) (Fig. 1), which is a triterpenoid derivative extracted from the bark of *Melia toosendan* Sieb et Zucc, was the strongest in enhancing α -IFN-induced ISRE reporter activation and the expression of interferon-stimulated genes (ISGs). TSN has been used as an anthelmintic vermifuge against ascaris (31). Although TSN has some other biological effects against toxin-producing anaerobic bacteria and against carcinoma cells (32, 45), antiviral activity has not been reported.

In this study, we showed, using an HCV replicon system, that TSN, with or without α -IFN, inhibits HCV replication in a cultured human hepatoma Huh7 cell line and that the combination of TSN and α -IFN shows synergistic effects on viral replication. We have investigated the mechanisms of action of

* Corresponding author. Mailing address: Department of Gastroenterology and Hepatology, Tokyo Medical and Dental University, 1-5-45 Yushima, Bunkyo-ku, Tokyo 113-8519, Japan. Phone: 81 3-5803-5877. Fax: 81 3-5803-0268. E-mail: nsakamoto.gast@tmd.ac.jp.

† Supplemental material for this article may be found at <http://aac.asm.org/>.

‡ T.W. and N.S. contributed equally to this work.

[∇] Published ahead of print on 28 March 2011.

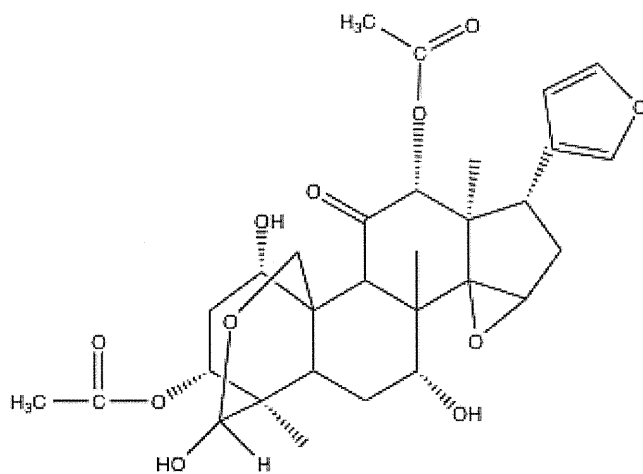


FIG. 1. Chemical structure of toosendanin.

TSN further and show that TSN induced activation of a component of interferon-stimulated gene factor 3 (ISGF3).

MATERIALS AND METHODS

Reagents. Alpha interferon was from Otsuka (Tokushima, Japan). TSN was from APIN Chemicals (Oxon, United Kingdom). Purity was over 77.32%. The designated concentration was achieved through dilution with cell culture medium (the final concentration of dimethyl sulfoxide [DMSO] in the medium was less than 0.3%). Beta-mercaptoethanol was from Wako (Osaka, Japan). The TSN used in this study was solubilized in DMSO.

Cells and cell culture. The human hepatoma cell line Huh7 was maintained in Dulbecco's modified Eagle's medium (Sigma, St. Louis, MO) supplemented with 10% fetal bovine serum at 37°C under 5% CO₂. To maintain cell lines carrying an HCV subgenomic replicon (Huh7/Rep-Feo), G418 (Nakalai Tesque, Kyoto, Japan) was added to the culture medium at a final concentration of 500 µg/ml.

HCV subgenomic replicon construct. The HCV subgenomic replicon plasmid pRep-Feo expresses a fusion gene comprising the firefly luciferase and neomycin phosphotransferase (37, 43). RNA was synthesized *in vitro* from the plasmid and transfected into Huh7 cells. After culture in the presence of G418, cell lines stably expressing the replicon were established.

Reporter constructs. We analyzed the effects of TSN, with or without α-IFN, on signal transduction of ISRE and nuclear factor-κappaB (NF-κappaB). A plasmid, pCIneo-Rluc-IRES-Fluc, was constructed to analyze HCV internal ribosome entry site (IRES)-mediated translation efficiency (23). Plasmids pISRE-TA-Luc and pNF-κappaB-Luc (Clontech Laboratories, Franklin Lakes, NJ) contained consensus motifs upstream of the firefly luciferase gene. A plasmid, pTA-Luc (Clontech), which lacks the enhancer element, was used to determine the background. Plasmid pRL-CMV (Promega, Madison, WI), which expresses the Renilla luciferase protein, was used for normalization of transfection efficiency (17).

ISRE reporter screening. Huh7 cells were seeded in 384-well plates at a density of 3.0 × 10³ cells/well. An ISRE-responsive firefly luciferase reporter was introduced using Lipofectamine 2000 (Invitrogen). Five hours after transfection, the cells were treated with 60,500 compounds from chemical libraries at a concentration of 3 µg/ml for 24 h and then treated with α-IFN at a concentration of 3 IU/ml. Six hours later, cells were lysed, and luciferase activities were quantified using a Steady Glo luciferase assay kit (Promega). The compounds were stored in 100% DMSO, and thus, the final concentration of DMSO was 0.3%. Z' factors were calculated as reported previously (46).

Luciferase assays and measurements of antiviral activity. Huh7/Rep-Feo cells were cultured with various concentrations of compound, such that the final DMSO concentration was 0.1%. Levels of HCV replication were quantified by internal luciferase assay after 48 h of culture. Luciferase activities were quantified using a luminometer (Promega) and the Bright-Glo luciferase assay system (Promega). Assays were performed in triplicate, and the results are expressed as mean percentage of the controls ± standard deviation (SD). The 50% effective concentration (EC₅₀) values were calculated using the probit method (2, 33). The

determination of EC₅₀s was performed three times, and EC₅₀s are presented as means ± SDs for each compound.

MTS assays. To evaluate cell viability, dimethylthiazol carboxymethoxyphenyl sulfophenyl tetrazolium (MTS) assays were performed using a Cell Titer 96 Aqueous One Solution cell proliferation assay (Promega) as previously reported (18, 22). Huh7/Rep-Feo cells and HCV-J6/JFH1-infected Huh7 cells were seeded in 96-well plates at a density of 8.0 × 10³ cells/well. After treatment, to analyze the therapeutic index with the same concentration of the drug and administration time, 20 µl/well of Cell Titer 96 Aqueous One Solution reagent was added to the cells cultured in a 96-well plate, the plate was incubated at 37°C for 60 min, and then the absorbance at 490 nm was recorded with a 96-well plate reader. The cells were analyzed when the growth became confluent. Cell viability was expressed as the concentration required for 50% cytotoxicity (CC₅₀). The drug selectivity index was calculated as CC₅₀/EC₅₀. All experiments were performed in triplicate.

Analyses of drug synergism. The effects of treatment of Huh7/Rep-Feo cells with α-IFN, alone and in combination with TSN, were analyzed by using isobologram analysis as described previously (27, 37). Dose inhibition curves of α-IFN and TSN were drawn with the two drugs used alone or in combination. In each drug combination, EC₅₀s for α-IFN and TSN were plotted against the fractional concentration of α-IFN and TSN on the x and y axes, respectively. A theoretical line of additivity is drawn between plots of the EC₅₀ for either drug that was used alone. The combined effects of the two drugs were considered additive, synergistic, or antagonistic if the plots of the drug combination were located on the line, below, or above the line of additivity, respectively.

HCV-J6/JFH1 cell culture. HCV-J6/JFH1 (21), which is a recombinant of HCV-JFH1 (42), was used. *In vitro*-synthesized HCV-J6/JFH1 RNA was transfected into naïve Huh7 cells (48), and the cells were cultured in the presence of drugs (34). Cellular viral RNA expression levels were measured using a real-time reverse transcription-PCR (RT-PCR) system.

Real-time RT-PCR analysis. Real-time RT-PCR was carried out as described previously (7). Total cellular RNA was extracted from cultured cells using Isogen (Nippon Gene, Tokyo, Japan), reverse transcribed, and subjected to real-time RT-PCR analyses. Expression of mRNA was quantified using TaqMan Universal PCR master mix, an ABI 7500 real-time PCR system (Applied Biosystems, CA), and a QuantiTect SYBR green PCR kit (Qiagen, CA). Some primers have been described elsewhere (30, 34). The primers used were -S (5'-TTT GAA ACA TCA AAG TTT TTC ACA GAC CTA-3'), -AS (5'-CAC AGT CAA GGT CCT TAG TAT TTC AGA TGT-3'), p56-S (5'-ACT TCG GAG AAA GGC ATT AGA TCT GGA AAG-3'), p56-AS (5'-TAA GGA CCT TGT CTC ACA GAT TTC TCA AAG-3'), Viperin-S (5'-GCT ACC AAG AGG AGA AAG CA-3'), Viperin-AS (5'-TTG ATC TTC TCC ATA CCA GC-3'), ISG20-S (5'-CTA CGA CAC GTC CAC TGA CAG G-3'), ISG20-AS (5'-CAT CGT TGC CCT CGC ATC TTC-3'), IRF9-S (5'-GCA GCA GCA GCC CTG AGC CAC AGG AAG TTA-3'), IRF9-AS (5'-TTA CCT GCA ACT TCG GTG GGG GGC CCA GGC-3'), IFNAR1-S (5'-CTT TCA AGT TCA GTG GCT CC-3'), IFNAR1-AS (5'-CAT CAG ATG CTT GTA CGC GGA G-3'), IFNAR2-S (5'-GCC AGA ATG CCT TCA TCG TCA G-3'), and IFNAR2-AS (5'-GTG AGT TGG TAC AAT GGA GTG G-3').

Western blotting. Twenty micrograms of total cell lysate was separated by SDS-PAGE and blotted onto a polyvinylidene fluoride Western blotting membrane. The membrane was incubated with the primary antibodies, followed by incubation with a peroxidase-labeled anti-IgG antibody, and were visualized by chemiluminescence using an enhance chemiluminescence Western blotting analysis system (Amersham Biosciences, Buckinghamshire, United Kingdom). The antibodies used were mouse anti-NS5A (BioDesign, ME), rabbit anti-signal transducer and activator of transcription 1 (anti-STAT1) p84/p91, rabbit anti-phospho-STAT1 (Tyr 701), rabbit anti-STAT2, rabbit anti-phospho-STAT2 (Tyr 690) (Santa Cruz, CA), and anti-beta-actin antibody (Sigma). NIH image software was used to analyze the densitometry of the Western blot analysis. Quantification of STAT phosphorylation was done using NIH image software, and the results correspond to the ratio between the phosphorylated STAT1 (p-STAT1) or p-STAT2 amount and the STAT1 or STAT2 amount normalized to the amount for the control without α-IFN and TSN. The results correspond to the ratio between the NS5A amount and the beta-actin amount normalized to the amount for the control without α-IFN and TSN.

Statistical analyses. Statistical analyses were performed using Student's *t* test. *P* values of less than 0.05 were considered statistically significant.

RESULTS

ISRE reporter screening. At the primary screening ($n = 1$), we defined a 1.5-fold induction in response to α -IFN to be a hit compound, and the hit rate was about 1%. At the secondary screening ($n = 4$), we selected the compound whose cps were 2 SDs larger than that for the drug used as a negative control, and the hit compound rate was 0.2% of the original library. Both assays were highly reproducible, and reflecting this, the Z' factor (46) for the ISRE reporter screen was 0.97.

TSN has activity against HCV RNA replication. Huh7/Rep-Feo cells were cultured with various concentrations of TSN, and the effect was measured using a luciferase assay. TSN caused a marked suppression of HCV RNA replication in a dose-dependent manner (Fig. 2A). The EC_{50} of TSN was 20.6 nM. In contrast, MTS assays showed that treatment with TSN had little effect on cellular viability and replication, with a CC_{50} of over 3 μ M and a selectivity index of more than 146. These results indicated that TSN had an effect against HCV RNA replication when it was used alone and that the effect was specific for HCV replication and not attributable to nonspecific cytotoxicity (Fig. 2B). Similarly, by Western blotting (Fig. 2C), the expression of HCV NS5A protein was shown to be reduced by corresponding amounts following treatment with TSN. To determine whether TSN suppresses HCV IRES-dependent translation, we used a Huh7 cell line that had been stably transfected with pCIneo-Rluc-IRES-Fluc (Fig. 2D). Treatment of these cells with TSN resulted in no significant change of the internal luciferase activities at concentrations of TSN that suppressed expression of the HCV replicon.

TSN increased ISRE reporter activity with α -IFN. Because we identified TSN originally through ISRE reporter-based drug screening, we analyzed the effects of TSN on the cellular responses to α -IFN following pretreatment with TSN. First, we treated ISRE-TA-Luc-transfected Huh7 cells with TSN and α -IFN simultaneously or pretreated the cells with 10 to 100 nM TSN at 24 or 48 h prior to α -IFN treatment. Luciferase assays were performed 6 h after addition of α -IFN at concentrations of 0.1 to 100 IU/ml (Fig. 3A and B). Treatment with TSN alone did not increase ISRE reporter activity. Similarly, simultaneous treatment with TSN and α -IFN did not enhance α -IFN-induced ISRE reporter activation more than treatment with α -IFN alone. In contrast, pretreatment with TSN 24 or 48 h before addition of α -IFN significantly increased ISRE activation compared to that achieved by treatment with α -IFN alone (Fig. 3A). On the basis of these results, we performed the subsequent experiments with addition of TSN 24 h before α -IFN treatment.

We next quantified the expression levels of ISGs, including those for 2',5'-oligoadenylate synthetase (25AS), MxA, protein kinase R, p56, viperin, and ISG20, which encode proteins with direct antiviral activity (14, 15, 25). Naïve Huh7 cells were treated with TSN for 24 h, followed by treatment with 100 IU/ml α -IFN for 24 h. The expression of each ISG was significantly elevated in a dose-dependent manner following pretreatment with TSN and α -IFN stimulation (Fig. 3C). These results indicated that TSN pretreatment significantly enhanced the cellular response to α -IFN-induced, ISRE-regulated expression of ISGs.

It has been reported that α -IFN receptor-mediated signaling

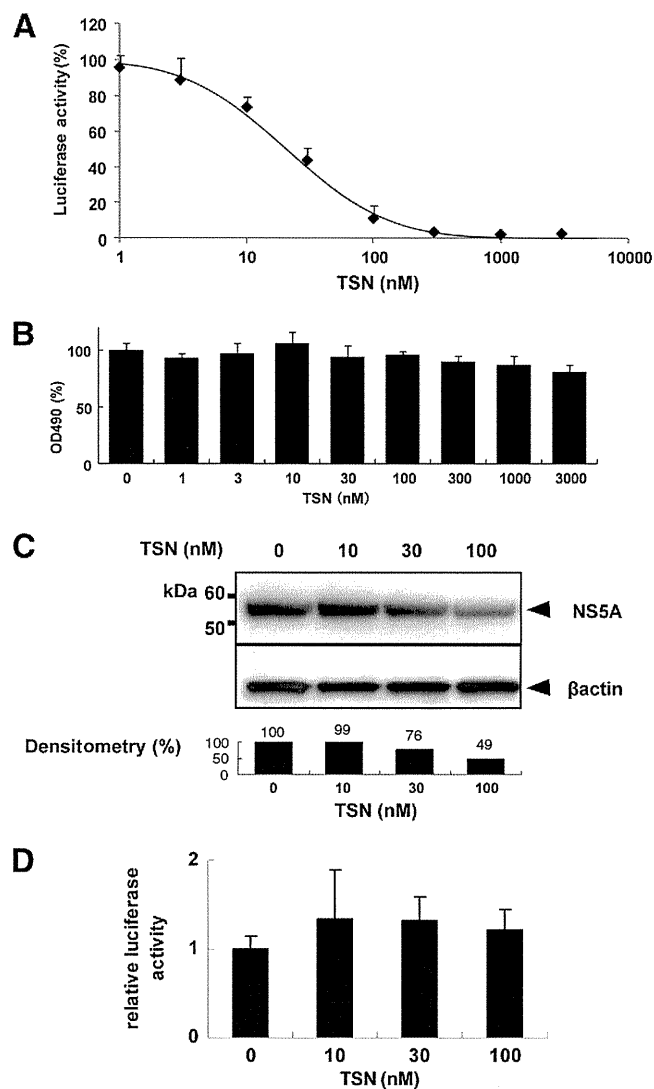


FIG. 2. Effect of TSN on expression of HCV replicon. (A) HCV replicon cells were treated with various concentrations of TSN for 48 h. Replication levels of HCV RNA were analyzed by luciferase assay. Bars indicate luciferase activities relative to that of the drug-negative control. (B) Cell viability was determined by MTS assay. Bars indicate the value relative to that of the drug-negative control. (C) Western blotting analyses. The expression of NS5A and beta-actin was detected using anti-NS5A and anti-beta-actin antibodies. Densitometry of NS5A protein was performed, and the result is indicated as a percentage of the result for the drug-negative control. The assay was repeated three times, and a representative result is shown. (D) A bicistronic reporter gene plasmid, pCIneo-Rluc-IRES-Fluc, was transfected into Huh7 cells. The cells were cultured with TSN at the concentrations indicated, and dual luciferase activities were measured after 24 h of treatment. Values are displayed as ratios of Fluc to Rluc. In panels A, B, and D, the assays were done in triplicate and repeated three times. Error bars indicate means \pm SDs.

cross talks with several alternative pathways, including the NF-kappaB, gamma IFN, phosphatidylinositol 3-kinase (PI3K), and mitogen-activated protein kinase (MAPK) pathways (9, 16, 24, 28). Therefore, we analyzed the effect of TSN on the signaling pathways indicated above. Cells were transfected with various reporter plasmids, including NF-kappaB, gamma

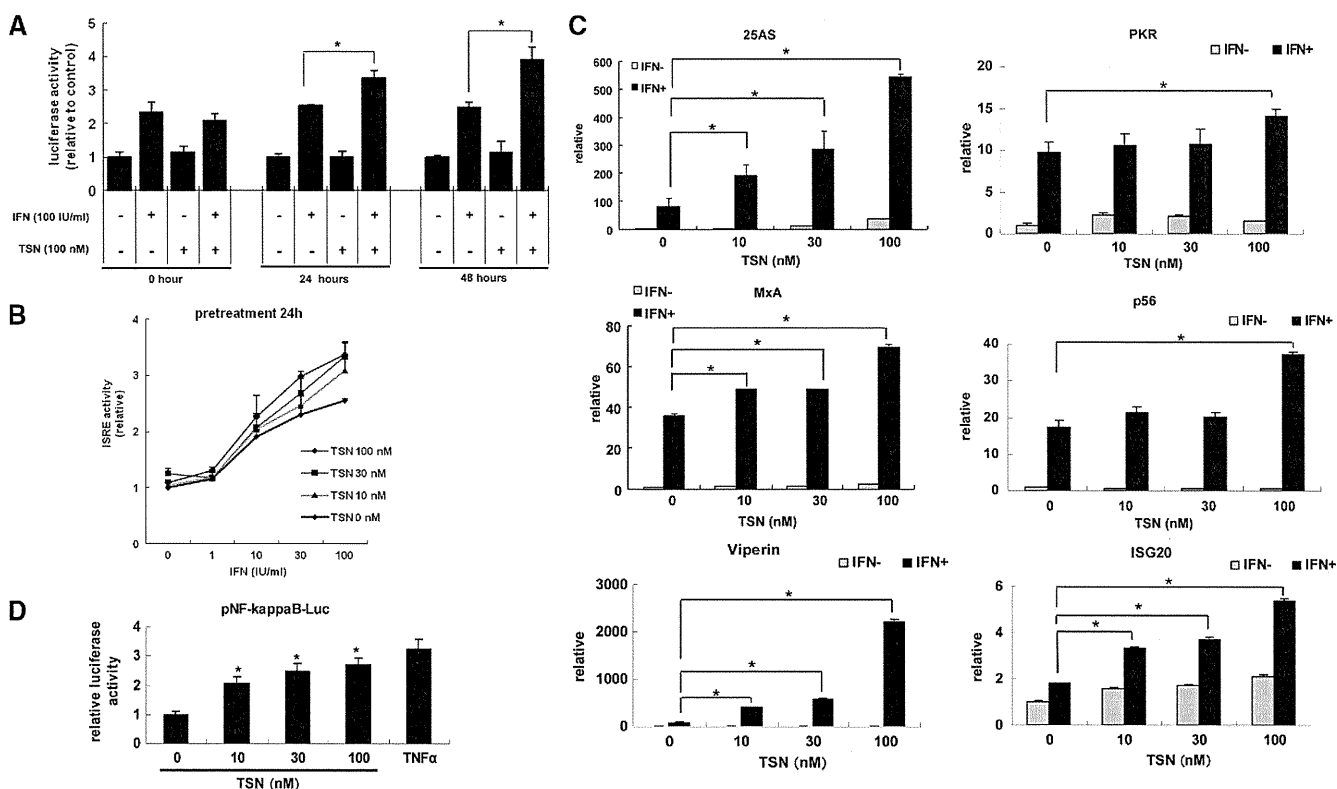


FIG. 3. ISRE reporter screening and aberrant pathway of α -IFN. (A) Pretreatment with TSN. Huh7 cells transfected with a reporter gene (pISRE-Luc and pRL-CMV) were pretreated with TSN (0 or 100 nM) for 0, 24, or 48 h, followed by treatment with α -IFN (0 or 100 IU/ml). Six hours later, the relative ISRE-luciferase activity ($n = 4$) was determined as described in Materials and Methods. The data are expressed as means \pm SDs and are a representative example of the data from three similar experiments. (B) Pretreatment with TSN at the concentrations indicated for 24 h, followed by treatment with α -IFN (0 to 100 IU/ml). The ISRE reporter assay was performed as described for panel A. (C) Type I IFN-induced antiviral ISG expression in Huh7 cells. Huh7 cells were treated with TSN for 24 h, followed by treatment with α -IFN at 100 IU/ml for 24 h. The total cellular RNA was then isolated for real-time RT-PCR analysis of the mRNAs of 25AS, MxA, p56, viperin, and ISG20. Beta-actin was used as a control. The data are expressed as means \pm SDs and are a representative example of data from three similar experiments. *, $P < 0.05$. (D) Analysis of aberrant pathways of α -IFN signaling under the influence of TSN. Promoter activities of NF-kappaB were analyzed by luciferase reporter assays. These cells were transfected with pNF-kappaB-TA-Luc, pTA-Luc which lacks the enhancer element and which was used as a negative control, and pRL-CMV to normalize transfection efficiency. At 24 h after transfection with these reporters, treatment with TSN (0, 10, 30, 100 nM) was carried out. After 24 h, the relative levels of induction of NF-kappaB activity for each treatment were calculated. TNF- α (50 ng/ml), which was used as a positive control for NF-kappaB, was added 6 h before analysis. The assays were done in triplicate and repeated three times. Error bars indicate means \pm SDs. *, $P < 0.05$.

interferon activation site (GAS), or activator protein 1 (AP1) Fluc plasmids. The reporter activities were measured after culture with or without TSN. As shown in Fig. 3D, there was no significant effect of TSN on GAS or AP1 reporter activities (data not shown). In contrast, NF-kappaB reporter activity was significantly elevated by TSN in a dose-dependent fashion.

Synergistic inhibitory effects of TSN and α -IFN on the replicon. We next assessed the effects of TSN combination with α -IFN on the intracellular replication of the HCV genome. Huh7/Rep-Feo cells were treated with various concentrations of TSN (0, 0.01, and 0.03 μ g/ml) and α -IFN (0 to 100 IU/ml). Replication of the HCV replicon was suppressed by pretreatment with TSN, followed by treatment with α -IFN, in a dose-dependent manner (Fig. 4A; see Fig. S1 in the supplemental material). The EC_{50} of α -IFN in the absence of TSN was 7.61 IU/ml, while that after pretreatment with 0.03 μ g/ml (41 nM) TSN was 3.16 IU/ml. These results indicated that pretreatment with TSN before α -IFN treatment is more effective in inhibiting HCV replication than treatment with α -IFN alone.

Subsequently, we conducted the following assay to determine whether TSN and α -IFN have a synergistic inhibitory effect on the replicon. The relative dose-inhibition curves of α -IFN were plotted for several concentrations of TSN and α -IFN. The curves shifted to the left with increasing concentrations of TSN (Fig. 4B), demonstrating that HCV replication was considerably reduced by the combination compared with that by either TSN or α -IFN alone. An MTS-based cell viability assay did not show significant cytotoxicity from TSN (Fig. 4C). Western blot analysis and densitometry of each blot showed results essentially identical to those from the luciferase assay (Fig. 4D).

We used isobologram analysis to determine whether the anti-HCV effect of TSN is synergistic with that of α -IFN (27, 37). Huh7/Rep-Feo cells were treated with a combination of α -IFN and TSN at an EC_{50} ratio of 1:0, 2:3, 1:4, or 0:1, and the dose-effect plots were drawn (Fig. 4E). The fractional EC_{50} s for α -IFN and TSN were plotted on the x and y axes, respectively, to generate an isobologram (Fig. 4F). Each plot showing

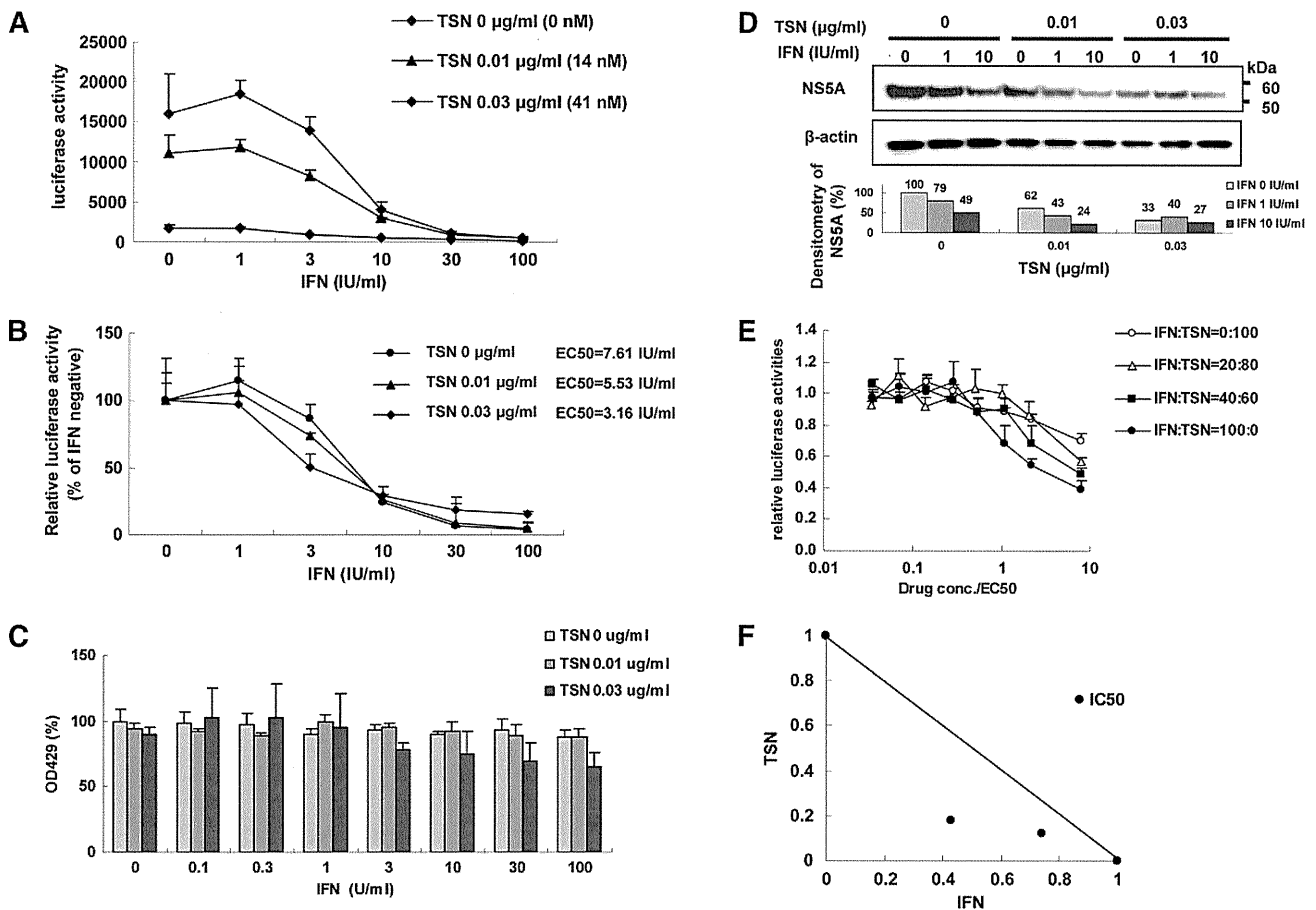


FIG. 4. Suppression of HCV RNA replication by TSN combined with α -IFN. (A and B) Luciferase activity (A, absolute value; B, relative value). Huh7/Rep-Feo cells, which constitutively express an HCV replicon, enable the quantification of replication levels through the measurement of luciferase activity. Absolute and relative dose-response curves in the presence of 24 h of pretreatment of various concentrations of TSN (0, 0.01, 0.03 μ g/ml) and α -IFN (0, 100 IU/ml). (A) Bars indicate luciferase activities. (B) Bars indicate luciferase activities relative to the activity of each α -IFN-negative control. Luciferase assays were performed in triplicate. Error bars indicate means \pm SDs. (C) MTS assay of Huh7/Rep-Feo cells cultured with the indicated concentrations of TSN and α -IFN. The assays were done in triplicate and repeated three times. Error bars indicate means \pm SDs. (D) Western blotting. Ten micrograms of total cellular protein was separated by polyacrylamide gel electrophoresis and transferred onto the membrane. Monoclonal anti-NS5A antibody or an anti-beta-actin antibody was used as the primary antibody. Densitometry of NS5A or beta-actin protein was performed and the result is indicated as a percentage of that for the drug-negative control. The assay was repeated three times, and representative results are shown. (E) Dose-inhibition curves of α -IFN and TSN when they were combined at the indicated ratios, adjusted by the EC_{50} of the individual drug. Assays were done in triplicate, and mean values were plotted and indicated as means \pm SDs. (F) Graphical representation of the isobologram analysis. For each drug combination in panel E, the EC_{50} s of α -IFN and TSN for inhibition of HCV replication were plotted against the fractional concentrations of α -IFN and TSN, which are indicated on the x and y axes, respectively. A theoretical line of additivity is drawn between the EC_{50} for each drug alone. All of the fractional EC_{50} plots for the TSN and α -IFN combinations fell below the line of additivity, indicating synergy.

the fractional EC_{50} of each drug ratio fell below the line showing additivity, indicating that the effect of the drug combination on intracellular HCV RNA replication was synergistic. The MTS values at the drug concentrations used in this isobologram analysis did not show any significant decrease, suggesting that the synergistic action of α -IFN and TSN on HCV replication is through their pharmacological effects and is not due to augmentation of cytotoxicity.

Suppression of HCV-J6/JFH1 infection by pretreatment of TSN with α -IFN. The inhibitory effects of pretreatment with TSN prior to α -IFN treatment demonstrated on HCV subgenomic replication were validated further using HCV-J6/JFH1 cell culture (21, 42). Various concentrations of TSN and α -IFN were added to HCV-J6/JFH1-infected Huh7 cells, and

intracellular HCV RNA was quantified after 48 h of incubation. As shown in Fig. 5A, TSN with or without α -IFN suppressed expression of intracellular HCV RNA in a dose-dependent manner. The EC_{50} s of α -IFN with TSN at 0, 10, and 30 nM were 4.71 IU/ml, 3.83 IU/ml, and 3.52 IU/ml, respectively. An MTS-based cell viability assay did not show significant cytotoxicity from TSN (Fig. 5B). These data indicate that pretreatment with TSN also augmented the α -IFN effect on the JFH1 system.

TSN upregulates ISGF3 in combination with α -IFN. Subsequently, we performed experiments to investigate the mechanisms of action of TSN. First, we quantified expression of alpha/beta IFN receptor subunit (IFNAR) 1 and IFNAR2 and the effect of TSN. Real-time RT-PCR analysis showed no

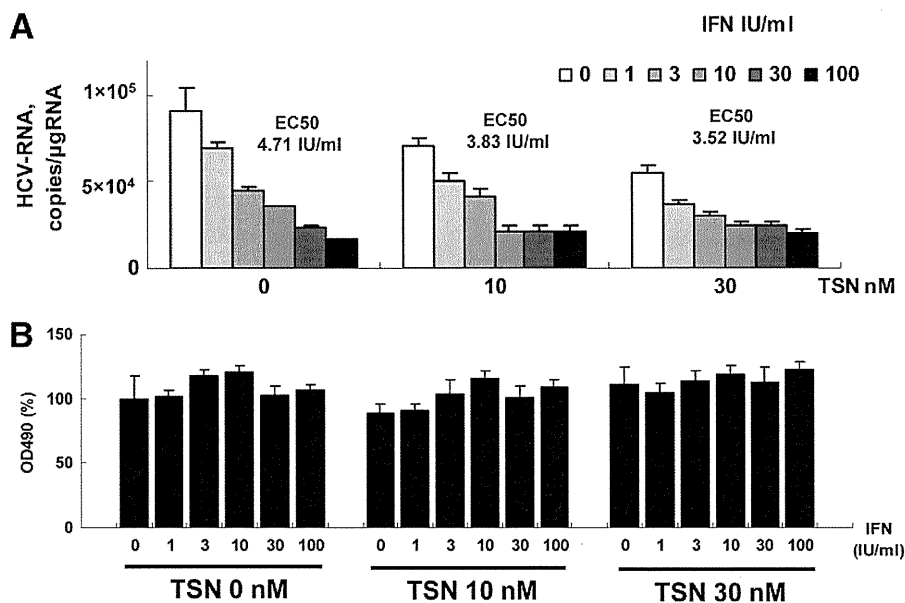


FIG. 5. Suppression of full HCV-J6/JFH1 replication by pretreatment of TSN with α -IFN. Ten micrograms of HCV-J6/JFH1 RNA was transfected into Huh7 cells. At 48 h after transfection, cells were pretreated with TSN for 24 h, followed by treatment with α -IFN (0, 1, 3, 10, 30, 100 IU/ml). At 48 h after α -IFN addition, cells were harvested. (A) Real-time RT-PCR analysis; (B) effect of pretreatment TSN with α -IFN on cell viability. MTS assays were performed 48 h after culture in the presence of pretreatment TSN with α -IFN. Bars indicate values relative to that of the drug-negative control. In panels A and B, the assays were done in triplicate and repeated three times. Error bars indicate means \pm SDs.

change in levels of IFNAR1 and IFNAR2 mRNA expression with or without TSN (Fig. 6).

Next, we investigated the ISGF3 components, STAT1, and STAT2, using Western blotting, and interferon regulatory factor 9 (IRF9), using real-time RT-PCR. Huh7 cells were treated with various concentrations of TSN or 0.01% DMSO. Twenty-four hours after TSN treatment, 100 IU/ml of α -IFN was added, and STATs and IRF9 were detected. Western blot analysis demonstrated that phosphorylated STAT1 and STAT2 levels were increased more by treatment with α -IFN and TSN than by α -IFN treatment alone (Fig. 7A and B). In addition, IRF9 mRNA expression was significantly higher following pretreatment with TSN prior to α -IFN therapy than by α -IFN monotherapy (Fig. 8). These findings are consistent with the hypothesis that TSN activates ISGF3 components in combination with α -IFN.

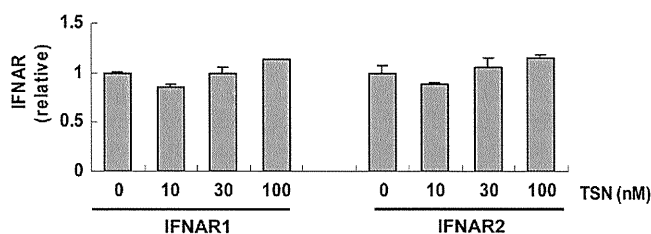


FIG. 6. IFNAR expression. Huh7 cells were pretreated with TSN for 24 h, followed by treatment with 100 IU/ml α -IFN for 6 h. The total cellular RNA was then isolated for real-time RT-PCR analysis of the mRNAs of IFNAR1 and IFNAR2. The assays were done in triplicate and repeated three times. The data are shown as means \pm SDs.

DISCUSSION

In this study, we investigated the molecular actions of TSN on HCV replication and on α -IFN-mediated cellular antiviral responses. Treatment of cells expressing an HCV subgenomic replicon with TSN alone specifically inhibited HCV replication with a selectivity index of more than 146 (Fig. 2). In addition, pretreatment of cells with TSN prior to addition of α -IFN augmented α -IFN receptor-mediated, ISRE-regulated gene expression (Fig. 3). Consistent with these findings, TSN pretreatment significantly enhanced the suppressive effects of α -IFN on the HCV replicon and HCV cell culture (Fig. 4 and 5). Finally, we demonstrated that the α -IFN-enhancing effects of TSN are through increased transcriptional activation of a component of ISGF3 (Fig. 7 and 8). Taken together, our results demonstrate that TSN is potentially an effective antiviral agent when it is used alone and especially when it is used in combination with α -IFN and that screening for such α -IFN-enhancing agents may identify promising antiviral therapeutics. Because TSN treatment alone or simultaneous treatment with TSN and α -IFN did not increase ISRE activity or augment α -IFN-mediated ISRE activation, TSN may affect α -IFN sensitivity by upregulating molecules that affect α -IFN receptor-mediated signaling without activating ISRE signaling directly.

Type I interferon plays a central role in eliminating viruses through its innate antiviral activity or following therapeutic application. Binding of α -IFNs to their receptors activates the Jak-STAT pathway to form a complex with ISGF3, which translocates to the nucleus, binds the ISRE located in the promoter/enhancer region of the ISGs, and activates expression of ISGs (28, 39, 40). In this study, we demonstrated that TSN enhanced α -IFN effects by upregulating ISGF3, which

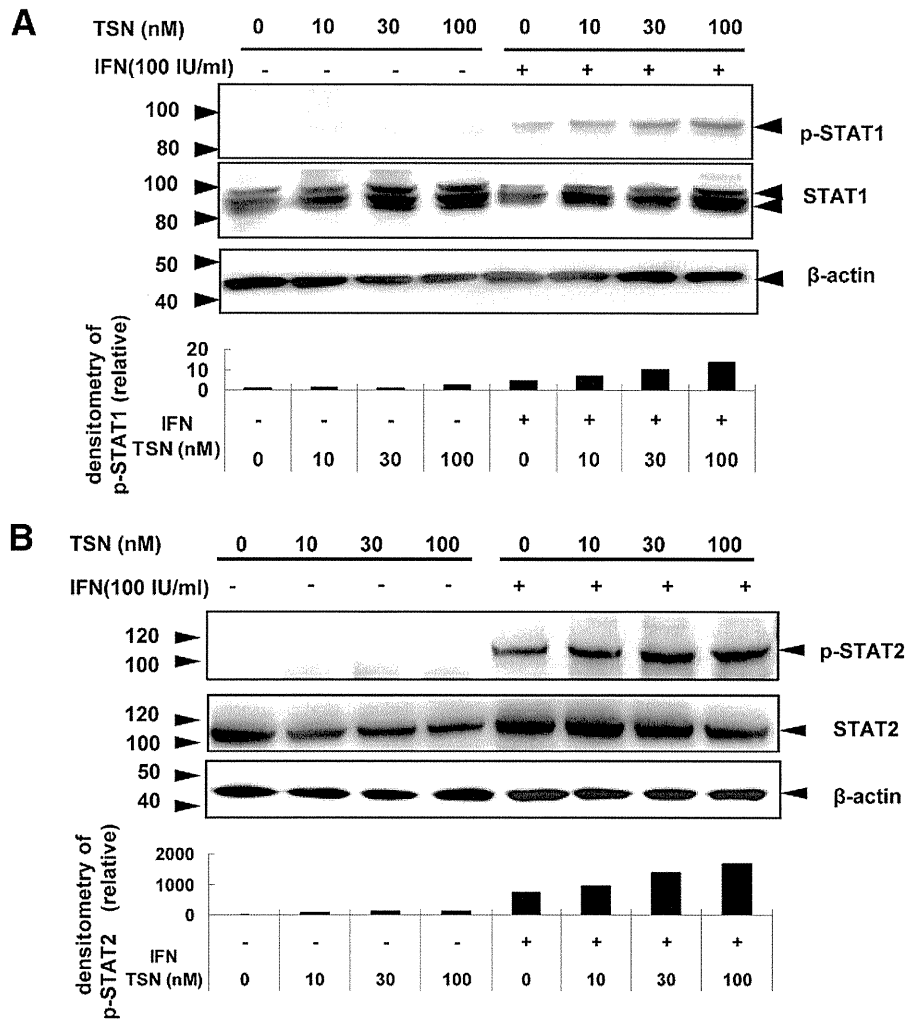


FIG. 7. TSN with α -IFN treatment of Huh7 cells increases phosphorylation of STAT1 and STAT2. (A) Western blotting. Alteration in the distribution of α -IFN-induced phosphorylation of STAT1 and STAT2 by TSN. Huh7 cells were treated with TSN or 0.01% DMSO for 24 h. After that, the cells were stimulated by 100 IU/ml α -IFN for 30 min. Cells were harvested, and the resulting lysates were analyzed for phosphorylated and total STAT1 or STAT2. The relative amounts of phosphorylated STAT1 or STAT2 were normalized to the amount of total STAT1 or STAT2 and expressed relative to the amount for the drug-negative control. The assay was repeated three times, and a representative result is shown.

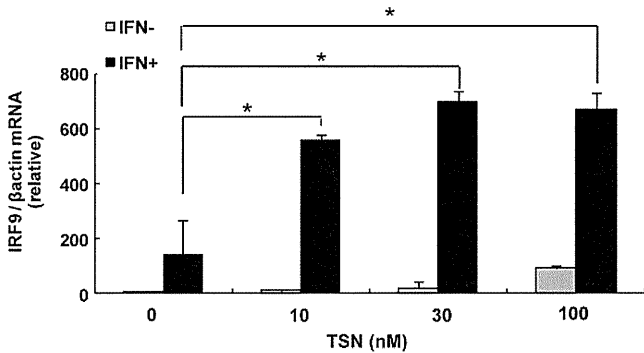


FIG. 8. IRF9 mRNA expression after combination treatment with TSN and α -IFN. Real-time RT-PCR analysis. Huh7 cells were treated with TSN for 24 h. After 6 h, the cells were stimulated by α -IFN (100 IU/ml). We used the method described in the legend to Fig. 6 to analyze the mRNA of IRF9. The assays were done in triplicate and repeated three times. Error bars indicate means \pm SDs. *, $P < 0.05$.

may cancel the suppressive effect of HCV gene products on the α -IFN signaling pathway.

In our study, it was not proved that increasing ISRE activities had direct relevance to inhibition of HCV replication. In Fig. 3C, we showed that TSN with α -IFN treatment had elevated the level of expression of mRNA of ISGs. Previous studies suggested that overexpression of known ISGs inhibited HCV replication in HCV replicon-containing Huh7 cells (13, 14). These findings may support the possibility that TSN had the potential to augment the α -IFN effect.

Other than the canonical Jak/STAT-mediated α -IFN signaling pathway, several alternative α -IFN pathways have been reported, including the NF-kappaB, gamma IFN, PI3K, and MAPK pathways (9, 16, 24, 28). We carried out reporter assays using NF-kappaB, AP1, and GAS reporter plasmid constructs and treated the cells with TSN. As shown in Fig. 3D, TSN activated NF-kappaB-regulated gene expression significantly. NF-kappaB is a sequence-specific transcription factor which

regulates the expression of numerous cellular and viral genes and plays important roles in inflammation, innate immune responses, tumorigenesis, and cell survival (3, 19). Activation of NF-kappaB is principally regulated by tumor necrosis factor alpha (TNF- α), Toll-like receptors (TLRs), and RIG-I, which may possibly be associated with the molecular mechanisms of TSN monotherapy. Horsmans et al. (12) and Agrawal and Kandimalla (1) reported that TLR7, -8, and -9 agonists have the ability to modulate TLR-mediated immune responses in targeting a broad range of disease vectors, including HCV, alone or in combination with other therapeutic agents. These reports support the hypothesis that activation of NF-kappaB may be one of the mechanisms of action of TSN.

It has been reported that TSN exhibits cytotoxic/antiproliferative potential at high concentrations (36, 47). In our study, the selectivity index of TSN against HCV was sufficient to ascertain that the antiviral effects are not simply due to the cytotoxicity of TSN. A recent study showed that a triterpenoid compound, dammarenolic acid, inhibits retrovirus, human immunodeficiency virus, simian immunodeficiency virus, murine leukemia virus, and respiratory syncytial virus infections *in vitro* (4) (5). We have analyzed the effects of dammarenolic acid on antiviral actions on Huh7/Rep-Feo cells, cytotoxicity, and ISRE reporter activation. However, dammarenolic acid did not inhibit HCV replication or enhanced α -IFN-induced ISRE activity (data not shown). These findings suggest that the anti-HCV and α -IFN enhancer effects are distinctive features of TSN among triterpenoid compounds. Hiasa et al. have reported that ME3738, a triterpenoid saponin, suppressed HCV replication through production of endogenous beta interferon (11). ME3738 is now in clinical trials for treatment of HCV-infected patients. Taking these findings together, despite reports on the cell-suppressive effect of triterpenoids, properly selected or designed compounds might be used as drugs against HCV infection.

Because the mechanisms of action of these triterpenoid compounds against these viruses are poorly understood, further investigation of the mechanism of action of TSN on HCV may be valuable to implement antiviral strategies against other viruses. It would be important to assess drug resistance after continuous treatment with TSN. There is no *in vitro* or *in vivo* report on resistance of TSN or cellular attenuation of responses to TSN. Such information, if any is found, would help elucidate the mechanism of action of TSN.

Given the current situation of limited therapeutic options against HCV, the search for more potent and less toxic antiviral drugs is needed to improve clinical anti-HCV chemotherapeutics. Several direct antiviral agents with activity against HCV are currently undergoing clinical trials. These include NS3 protease inhibitors and NS5B polymerase inhibitors (41). However, the frequent emergence of drug-resistant viruses is a major weakness of such agents (20). Our results indicate that TSN is also effective at suppressing HCV infection and replication. Future studies with TSN, its derivatives, and other chemicals that target the α -IFN pathway could be directed toward developing a new class of antiviral treatment regimens and drugs.

ACKNOWLEDGMENTS

We thank Frank Chisari for providing Huh7.5.1 cells, Charles Rice for providing plasmid pJ6/JFH1full, and Takaji Wakita for providing plasmid pJFH1full.

This study was supported by grants from the Ministry of Education, Culture, Sports, Science and Technology of Japan, the Japan Society for the Promotion of Science, the Ministry of Health, Labor and Welfare of Japan, the Japan Health Sciences Foundation, the National Institute of Biomedical Innovation, and the Miyakawa Memorial Research Foundation.

REFERENCES

1. Agrawal, S., and E. R. Kandimalla. 2007. Synthetic agonists of Toll-like receptors 7, 8 and 9. *Biochem. Soc. Trans.* **35**:1461-1467.
2. Bailey, M., N. A. Williams, A. D. Wilson, and C. R. Stokes. 1992. PROBIT: weighted probit regression analysis for estimation of biological activity. *J. Immunol. Methods* **153**:261-262.
3. Baldwin, A. S., Jr. 2001. Series introduction: the transcription factor NF-kappaB and human disease. *J. Clin. Invest.* **107**:3-6.
4. Esimone, C. O., et al. 2008. Potential anti-respiratory syncytial virus lead compounds from *Aglaia* species. *Pharmazie* **63**:768-773.
5. Esimone, C. O., et al. Dammarenolic acid, a secodammarane triterpenoid from *Aglaia* sp. shows potent anti-retroviral activity *in vitro*. *Phytomedicine* **17**:540-547.
6. Fried, M. W., et al. 2002. Peginterferon alfa-2a plus ribavirin for chronic hepatitis C virus infection. *N. Engl. J. Med.* **347**:975-982.
7. Funaoaka, Y., et al. Analysis of interferon signaling by infectious hepatitis C virus clones with substitutions of core amino acids 70 and 91. *J. Virol.*, in press.
8. Ge, D., et al. 2009. Genetic variation in IL28B predicts hepatitis C treatment-induced viral clearance. *Nature* **461**:399-401.
9. Goodbourn, S., L. Didcock, and R. E. Randall. 2000. Interferons: cell signalling, immune modulation, antiviral response and virus countermeasures. *J. Gen. Virol.* **81**:2341-2364.
10. Hadziyannis, S. J., et al. 2004. Peginterferon-alpha2a and ribavirin combination therapy in chronic hepatitis C: a randomized study of treatment duration and ribavirin dose. *Ann. Intern. Med.* **140**:346-355.
11. Hiasa, Y., et al. 2008. Hepatitis C virus replication is inhibited by 22beta-methoxyolean-12-ene-3beta, 24(4beta)-diol (ME3738) through enhancing interferon-beta. *Hepatology* **48**:59-69.
12. Horsmans, Y., et al. 2005. Isatoribine, an agonist of TLR7, reduces plasma virus concentration in chronic hepatitis C infection. *Hepatology* **42**:724-731.
13. Itsui, Y., et al. 2009. Antiviral effects of the interferon-induced protein guanylate binding protein 1 and its interaction with the hepatitis C virus NS5B protein. *Hepatology* **50**:1727-1737.
14. Itsui, Y., et al. 2006. Expressional screening of interferon-stimulated genes for antiviral activity against hepatitis C virus replication. *J. Viral Hepat.* **13**:690-700.
15. Jiang, D., et al. 2008. Identification of three interferon-inducible cellular enzymes that inhibit the replication of hepatitis C virus. *J. Virol.* **82**:1665-1678.
16. Kalvakolanu, D. V. 2003. Alternate interferon signaling pathways. *Pharmacol. Ther.* **100**:1-29.
17. Kanazawa, N., et al. 2004. Regulation of hepatitis C virus replication by interferon regulatory factor 1. *J. Virol.* **78**:9713-9720.
18. Karakama, Y., et al. 2010. Inhibition of hepatitis C virus replication by a specific inhibitor of serine-arginine-rich protein kinase. *Antimicrob. Agents Chemother.* **54**:3179-3186.
19. Karin, M., and A. Lin. 2002. NF-kappaB at the crossroads of life and death. *Nat. Immunol.* **3**:221-227.
20. Kuntzen, T., et al. 2008. Naturally occurring dominant resistance mutations to hepatitis C virus protease and polymerase inhibitors in treatment-naive patients. *Hepatology* **48**:1769-1778.
21. Lindenbach, B. D., et al. 2005. Complete replication of hepatitis C virus in cell culture. *Science* **309**:623-626.
22. Mishima, K., et al. 2010. Cell culture and *in vivo* analyses of cytopathic hepatitis C virus mutants. *Virology* **405**:361-369.
23. Nakagawa, M., et al. 2005. Suppression of hepatitis C virus replication by cyclosporin A is mediated by blockade of cyclophilins. *Gastroenterology* **129**:1031-1041.
24. Randall, R. E., and S. Goodbourn. 2008. Interferons and viruses: an interplay between induction, signalling, antiviral responses and virus countermeasures. *J. Gen. Virol.* **89**:1-47.
25. Sadler, A. J., and B. R. Williams. 2008. Interferon-inducible antiviral effectors. *Nat. Rev. Immunol.* **8**:559-568.
26. Sakamoto, N., and M. Watanabe. 2009. New therapeutic approaches to hepatitis C virus. *J. Gastroenterol.* **44**:643-649.
27. Sakamoto, N., et al. 2007. Bone morphogenetic protein-7 and interferon-alpha synergistically suppress hepatitis C virus replicon. *Biochem. Biophys. Res. Commun.* **357**:467-473.

28. Samuel, C. 2001. Antiviral actions of interferons. *Clin. Microbiol. Rev.* **14**:778–809.
29. Sangiovanni, A., et al. 2006. The natural history of compensated cirrhosis due to hepatitis C virus: a 17-year cohort study of 214 patients. *Hepatology* **43**:1303–1310.
30. Sekine-Osajima, Y., et al. 2008. Development of plaque assays for hepatitis C virus-JFH1 strain and isolation of mutants with enhanced cytopathogenicity and replication capacity. *Virology* **371**:71–85.
31. Shi, Y. L., and M. F. Li. 2007. Biological effects of toosendanin, a triterpenoid extracted from Chinese traditional medicine. *Prog. Neurobiol.* **82**:1–10.
32. Shi, Y. L., and Z. F. Wang. 2004. Cure of experimental botulism and anti-botulismic effect of toosendanin. *Acta Pharmacol. Sin.* **25**:839–848.
33. Soothill, J. S., R. Ward, and A. J. Girling. 1992. The IC50: an exactly defined measure of antibiotic sensitivity. *J. Antimicrob. Chemother.* **29**:137–139.
34. Suda, G., et al. IL-6-mediated intersubgenotypic variation of interferon sensitivity in hepatitis C virus genotype 2a/2b chimeric clones. *Virology* **407**:80–90.
35. Suppiah, V., et al. 2009. IL28B is associated with response to chronic hepatitis C interferon-alpha and ribavirin therapy. *Nat. Genet.* **41**:1100–1104.
36. Tada, K., M. Takido, and S. Kitanaka. 1999. Limonoids from fruit of *Melia toosendan* and their cytotoxic activity. *Phytochemistry* **51**:787–791.
37. Tanabe, Y., et al. 2004. Synergistic inhibition of intracellular hepatitis C virus replication by combination of ribavirin and interferon-alpha. *J. Infect. Dis.* **189**:1129–1139.
38. Tanaka, Y., N. Nishida, M. Sugiyama, K. Tokunaga, and M. Mizokami. Lambda-interferons and the single nucleotide polymorphisms: a milestone to tailor-made therapy for chronic hepatitis C. *Hepatol. Res.* **40**:449–460.
39. Taniguchi, T., K. Ogasawara, A. Takaoka, and N. Tanaka. 2001. IRF family of transcription factors as regulators of host defense. *Annu. Rev. Immunol.* **19**:623–655.
40. Taniguchi, T., and A. Takaoka. 2002. The interferon-alpha/beta system in antiviral responses: a multimodal machinery of gene regulation by the IRF family of transcription factors. *Curr. Opin. Immunol.* **14**:111–116.
41. Thompson, A. J., and J. G. McHutchison. 2009. Antiviral resistance and specifically targeted therapy for HCV (STAT-C). *J. Viral Hepat.* **16**:377–387.
42. Wakita, T., et al. 2005. Production of infectious hepatitis C virus in tissue culture from a cloned viral genome. *Nat. Med.* **11**:791–796.
43. Yokota, T., et al. 2003. Inhibition of intracellular hepatitis C virus replication by synthetic and vector-derived small interfering RNAs. *EMBO Rep.* **4**:602–608.
44. Zeuzem, S., et al. 2000. Peginterferon alfa-2a in patients with chronic hepatitis C. *N. Engl. J. Med.* **343**:1666–1672.
45. Zhang, B., Z. F. Wang, M. Z. Tang, and Y. L. Shi. 2005. Growth inhibition and apoptosis-induced effect on human cancer cells of toosendanin, a triterpenoid derivative from Chinese traditional medicine. *Invest. New Drugs* **23**:547–553.
46. Zhang, J. H., T. D. Chung, and K. R. Oldenburg. 1999. A simple statistical parameter for use in evaluation and validation of high throughput screening assays. *J. Biomol. Screen.* **4**:67–73.
47. Zhang, Y., et al. 2008. Roles of reactive oxygen species and MAP kinases in the primary rat hepatocytes death induced by toosendanin. *Toxicology* **249**:62–68.
48. Zhong, J., et al. 2005. Robust hepatitis C virus infection in vitro. *Proc. Natl. Acad. Sci. U. S. A.* **102**:9294–9299.



Contents lists available at ScienceDirect

Biochemical and Biophysical Research Communications

journal homepage: www.elsevier.com/locate/ybbrc

Cholestatic liver fibrosis and toxin-induced fibrosis are exacerbated in matrix metalloproteinase-2 deficient mice

Izumi Onozuka^{a,1}, Sei Kakinuma^{a,b,*}, Akihide Kamiya^c, Masato Miyoshi^d, Naoya Sakamoto^{a,b}, Kei Kiyohashi^a, Takako Watanabe^a, Yusuke Funaoka^a, Mayumi Ueyama^a, Mina Nakagawa^a, Naohiko Koshikawa^e, Motoharu Seiki^e, Hiromitsu Nakauchi^c, Mamoru Watanabe^{a,*}

^a Department of Gastroenterology and Hepatology, Tokyo Medical and Dental University, Japan

^b Department for Hepatitis Control, Tokyo Medical and Dental University, Japan

^c Division of Stem Cell Therapy, Institute of Medical Science, The University of Tokyo, Japan

^d School of Medicine, Tokyo Medical and Dental University, Japan

^e Division of Cancer Cell Research, Institute of Medical Science, The University of Tokyo, Japan

ARTICLE INFO

Article history:

Received 25 January 2011

Available online 12 February 2011

Keywords:

Bile duct ligation
Carbon tetrachloride
PDGF receptor
TIMP1
TGF β

ABSTRACT

Matrix metalloproteinase (MMP) plays an important role in homeostatic regulation of the extracellular environment and degradation of matrix. During liver fibrosis, several MMPs, including MMP-2, are up-regulated in activated hepatic stellate cells, which are responsible for exacerbation of liver cirrhosis. However, it remains unclear how loss of MMP-2 influences molecular dynamics associated with fibrogenesis in the liver. To explore the role of MMP-2 in hepatic fibrogenesis, we employed two fibrosis models in mice; toxin (carbon tetrachloride, CCl₄)-induced and cholestasis-induced fibrosis. In the chronic CCl₄ administration model, MMP-2 deficient mice exhibited extensive liver fibrosis as compared with wild-type mice. Several molecules related to activation of hepatic stellate cells were up-regulated in MMP-2 deficient liver, suggesting that myofibroblastic change of hepatic stellate cells was promoted in MMP-2 deficient liver. In the cholestasis model, fibrosis in MMP-2 deficient liver was also accelerated as compared with wild type liver. Production of tissue inhibitor of metalloproteinase 1 increased in MMP-2 deficient liver in both models, while transforming growth factor β , platelet-derived growth factor receptor and MMP-14 were up-regulated only in the CCl₄ model. Our study demonstrated, using 2 experimental murine models, that loss of MMP-2 exacerbates liver fibrosis, and suggested that MMP-2 suppresses tissue inhibitor of metalloproteinase 1 up-regulation during liver fibrosis.

© 2011 Elsevier Inc. All rights reserved.

1. Introduction

The incidence of liver cirrhosis and cirrhosis-related cancer has steadily increased. Insight into the pathophysiology of hepatic fibrogenesis and fibrolysis is of particular importance. Accumulating evidences has indicated that matrix metalloproteinases

(MMPs) play an essential role in hepatic fibrogenesis [1]. Traditional substrates of MMPs are components of the extracellular matrix (ECM), such as collagen, laminin, and fibronectin [2]. More than 20 enzymes have been identified as MMPs in mammals. In healthy liver, homeostasis of the ECM is maintained by precisely regulated turnover controlled by MMPs and tissue inhibitors of metalloproteinases (TIMPs) [1]. Hepatic stellate cells activated in chronically damaged liver disrupt this regulation by synthesizing a large amount of ECM, including collagen and proteoglycan, followed by production of MMPs and TIMPs [3]. It has been reported that the hepatic expression of MMP-1, -2, -7 and -14 is steadily increased with disease progression, and that the expression of MMP-9, -11 and -13 is transiently elevated in hepatitis C virus-induced cirrhosis [4]. Up-regulation of MMPs and TIMPs during liver fibrogenesis has been observed in rodent models of liver fibrosis. In chronic toxin (carbon tetrachloride, CCl₄)-induced rat liver fibrosis, production of MMP-2, -9, and -14 is increased during the accumulation of fibrotic scarring in the liver, and hepatic stellate cells

Abbreviations: ALT, alanine aminotransferase; α SMA, α smooth muscle actin; AST, aspartate aminotransferase; BDL, bile duct ligation; CCl₄, carbon tetrachloride; ECM, extracellular matrix; GGT, γ -glutamyltranspeptidase; MMP, matrix metalloproteinase; MMP-2 KO, MMP-2 deficient; PDGF, platelet-derived growth factor; T-Bil, total bilirubin; TIMP, tissue inhibitor of metalloproteinase; TGF, transforming growth factor; WT, wild type.

* Corresponding authors at: Department of Gastroenterology and Hepatology, Tokyo Medical and Dental University, 1-5-45 Yushima, Bunkyo-ku, Tokyo 1138519, Japan. Fax: +81 3 5803 0268.

E-mail addresses: skakinuma.gast@tmd.ac.jp (S. Kakinuma), mamoru.gast@tmd.ac.jp (M. Watanabe).

¹ These authors contributed equally to this study.

appear to be the predominant source [5–7]. MMPs degrade the ECM, and yet loss of MMP activity does not always induce fibrogenesis *in vivo*, because MMP functions are associated with regulation of several inflammatory cytokines [8].

MMP-2 is a 72-kDa zinc-dependent type IV collagenase, and the activation of proMMP-2 is controlled by MMP-14 and TIMP2 [9]. In the rat CCl₄-induced fibrosis model, expression of MMP-2 increase up to 7–12 times as compared with that of controls, with the expression rate being maximal at an intermediate stage of fibrosis [5]. During the aggressive phase of CCl₄-induced liver fibrosis, MMP-2 is predominantly produced from myofibroblasts derived from hepatic stellate cells [7]. MMP-2 expression has been shown to increase during spontaneous recovery from cirrhosis in a rat toxin-induced fibrosis model [10]. The proteolytic activity of MMP-2 is increased in cholestasis-induced liver fibrosis models in rats and mice [6,11]. These studies indicate that MMP-2 regulates both liver fibrogenesis and fibrolysis. However, it remains unclear how MMP-2 functions during hepatic fibrogenesis in the liver *in vivo*, and the functional correlations between MMP and TIMP expression with liver fibrogenesis has not yet been fully elucidated.

In this study, to clarify the pivotal role of MMP-2 during liver fibrosis, we studied fibrotic changes in the liver of MMP-2 deficient (MMP-2 KO) mice using two types of fibrosis models; toxin (CCl₄)-induced fibrosis and cholestasis-induced fibrosis. In both models, liver fibrosis was accelerated in MMP-2 KO mice as compared with wild type (WT) littermates. Type I collagen expression and TIMP1 production were up-regulated in MMP-2 KO livers in both models. Our data indicated that MMP-2 plays an essential role in suppressing fibrotic changes in the liver arising from chemical or cholestatic damage.

2. Materials and methods

2.1. Animals

MMP-2 deficient (MMP-2 KO) mice on C57BL/6J background were originally generated by Itoh et al. [12]. MMP-2 KO mice and wild type (WT) littermates were produced by crossbreeding MMP-2 heterozygous mice. All animals were treated under the guidelines of the Institute of Medical Science, University of Tokyo and those of Tokyo Medical and Dental University.

2.2. Liver fibrosis induced by chronic CCl₄ administration

To induce hepatic fibrosis in mice, 6-week-old female MMP-2 KO and WT mice ($n = 4$ per group) were intraperitoneally injected with 10% CCl₄ (2 ml/kg body weight, Wako Pure Chemical Industries, Osaka, Japan) dissolved in olive oil (Wako) twice weekly for 12 weeks. Negative control mice were injected with 100% olive oil alone twice weekly for 12 weeks.

2.3. Liver fibrosis induced by bile duct ligation (BDL)

To induce fibrosis by cholestasis, 8-week-old female MMP-2 KO and WT mice ($n = 4$ per group) underwent common bile duct ligation under anesthesia as previously described [13]. Mice were sacrificed 2 weeks after the operation.

2.4. Blood biochemical tests

Peripheral blood of MMP-2 KO and WT mice in the BDL group was collected and assayed for total bilirubin (T-Bil), alanine aminotransferase (ALT), aspartate aminotransferase (AST), and γ -glutamyl-transpeptidase (GGT) using a Fuji DRI-Chem 3000 system (Fujifilm, Tokyo, Japan).

2.5. Immunohistological analysis

Fresh livers were snap-frozen in OCT compound and sectioned 8- μ m thick. The protocols for immunostaining has been described previously [14]. Immunohistological analysis was performed using mouse anti- α smooth muscle actin (α SMA) antibody (Sigma, St. Louis, MO, USA). For each analysis, addition of an appropriate immune serum provided a negative control.

2.6. Western blot analyses

Samples of liver tissue were homogenized in RIPA buffer. The protocols for western blot analyses have been described previously [15]. Western blot analyses were performed with liver homogenates (50 μ g protein) using anti- α SMA Ab (Sigma, 1:2000 dilution), anti-MMP9 antibody (Chemicon, Billerica, MA, USA, 1:1000 dilution), anti-MMP14 antibody (Abcam, Cambridge, MA, USA, 1:500 dilution), anti-TIMP1 antibody (Abcam, 1:1000 dilution), anti-TIMP2 antibody (Cell Signaling, Danvers, MA, USA, 1:500 dilution), or anti- β -actin antibody. Membrane pictures of immunoblots were quantified using ImageJ software (<http://rsb.info.nih.gov/ij/>).

Supplementary materials and methods are described in supplementary file.

3. Results

3.1. CCl₄-induced hepatic fibrosis in MMP-2 KO mice

We initially studied liver fibrosis induced by chronic CCl₄ administration in WT and MMP-2 KO mice. To induce extensive liver fibrosis, CCl₄ was injected twice weekly for 12 weeks. Damage of hepatocytes in MMP-2 KO livers was very severe (Fig. S1). Sirius red staining of KO livers demonstrated that CCl₄-induced fibrosis was severe in comparison with WT livers (Fig. 1A). Marked porto-central and porto-portal fibrosis was observed in the liver of MMP-2 KO mice treated with CCl₄. The fibrosis areas, quantified using an image analysis system, were significantly increased in MMP-2 KO livers as compared with WT livers (Fig. 1B). Following chronic CCl₄ administration, a 2-fold increase in fibrosis area was observed in MMP-2 KO livers as compared with WT livers.

3.2. Increased hepatic production of α SMA in MMP-2 KO mice treated with CCl₄

To assess whether the activation of hepatic stellate cells is promoted in MMP-2 KO mice with CCl₄-induced liver fibrosis, we examined hepatic α SMA production, which is a representative marker for myofibroblasts. Immunohistological analysis showed that α SMA-positive areas in the liver were much larger in CCl₄-treated MMP-2 KO mice than in CCl₄-treated WT mice (Fig. 1C). α SMA-positive areas quantified using an image analysis system were significantly increased in MMP-2 KO livers (Fig. 1D). Immunoblot analysis indicated that α SMA production was markedly increased in the livers of CCl₄-treated WT and MMP-2 KO mice as compared with vehicle (olive oil)-treated WT and MMP-2 KO mice, respectively. Hepatic α SMA production was higher in CCl₄-treated MMP-2 KO mice as compared with CCl₄-treated WT mice (Fig. 1E). Quantitative analysis using densitometry demonstrated that hepatic level of α SMA protein was significantly higher in CCl₄-treated MMP-2 KO mice than in CCl₄-treated WT mice (Fig. 1F). These data suggest that the activation of hepatic stellate cells was promoted in MMP-2 KO liver as compared with WT liver during liver fibrosis induced by chronic CCl₄ administration.

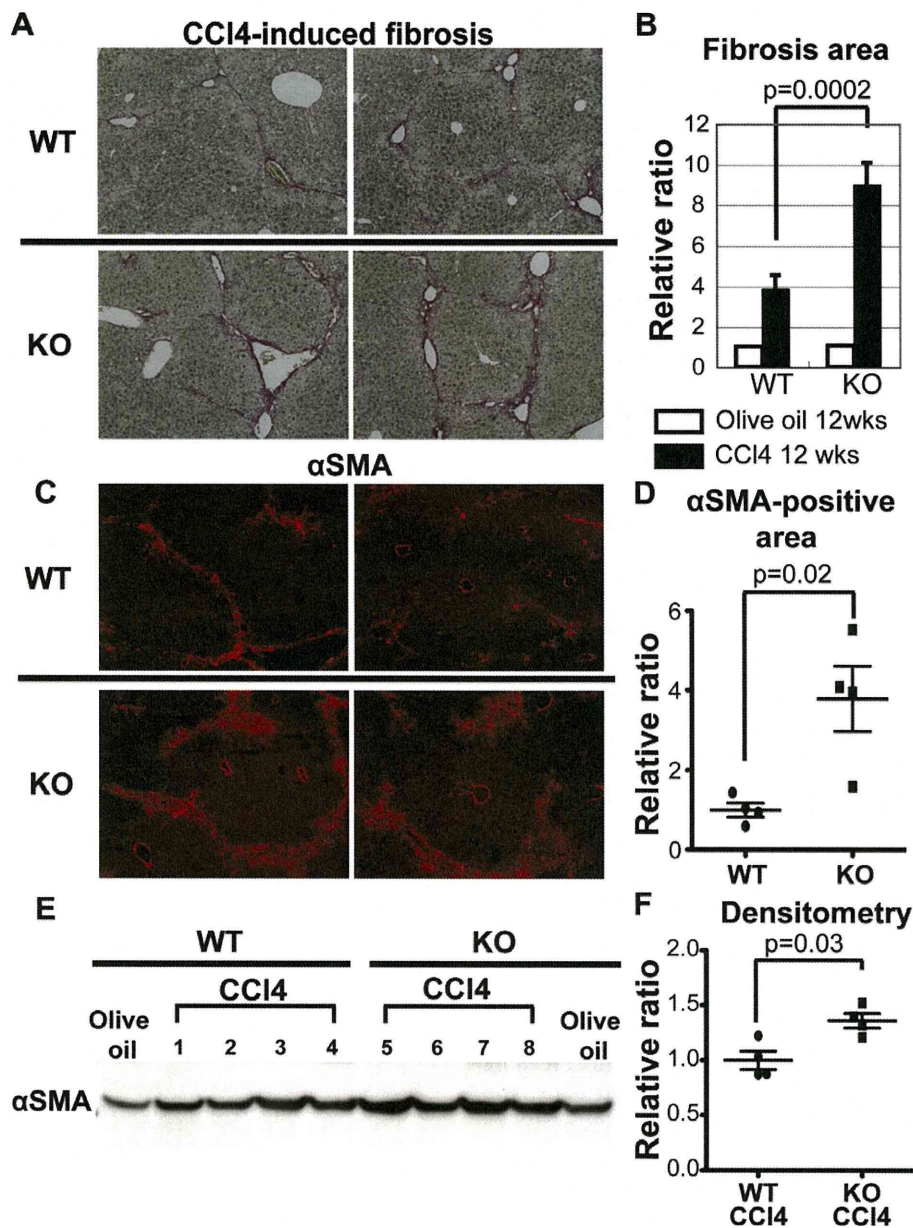


Fig. 1. CCI4-induced liver fibrosis is promoted in MMP-2 deficient (KO) mice. (A) Representative photographs of Sirius red staining in the livers of CCI4-treated mice. (B) Ratio of overall fibrosis area (red areas in Sirius red staining) relative to olive oil-treated WT mice. Data represent means \pm SD. (C) Representative images of α SMA immunostaining in the livers of CCI4-treated mice. (D) Areas immunostained with α SMA antibody, quantified using an image analysis system, were significantly increased in CCI4-treated MMP-2 KO mice as compared with WT mice. Values represent the ratio relative to the mean for CCI4-treated WT mice. Bars represent means \pm SEM. (E) Immunoblot analysis of α SMA in the liver of MMP-2 KO and WT mice. Mice 1, 2, 3, and 4 were CCI4-treated WT. Mice 5, 6, 7, and 8 were CCI4-treated MMP-2 KOs. (F) Hepatic α SMA protein quantified using densitometry was significantly increased in CCI4-treated MMP-2 KO mice as compared with WT mice. Values represent the ratio relative to the mean for CCI4-treated WT mice. Bars represent means \pm SEM.

3.3. Hepatic expression of fibrosis-related molecules in CCI4-treated MMP-2 KO mice

To explore the molecular mechanism underlying the differences between WT and MMP-2 KO mice in response to CCI4-induced fibrosis, we analyzed the expression of molecules related to the promotion of liver fibrosis. Quantitative RT-PCR analysis showed that the hepatic expression of type I collagen in CCI4-treated MMP-2 KO mice was 4-fold higher than that in CCI4-treated WT mice (Fig. 2A). In addition, hepatic expression of transforming growth factor (TGF) β 1 and platelet-derived growth factor (PDGF) receptor was up-regulated in CCI4-treated MMP-2 KO mice,

whereas that of TGF β receptor was comparable between CCI4-treated MMP-2 KO mice and CCI4-treated WT mice (Fig. 2A).

Immunoblot analysis showed that hepatic levels of MMP-9, MMP-14, TIMP1, and TIMP2 protein were increased in CCI4-treated WT mice relative to vehicle-treated mice, indicating that production of fibrosis-related molecules was up-regulated in our experimental model (Fig. 2B). Production of MMP-9, MMP-14, TIMP1 and TIMP2 in the liver was comparable between vehicle-treated WT mice and vehicle-treated KO mice (Fig. 2B). Quantitative analysis using densitometry also showed that hepatic production of MMP-14 and TIMP1 was significantly higher in CCI4-treated MMP-2 KO mice than in CCI4-treated WT mice (Fig. 2C). Hepatic

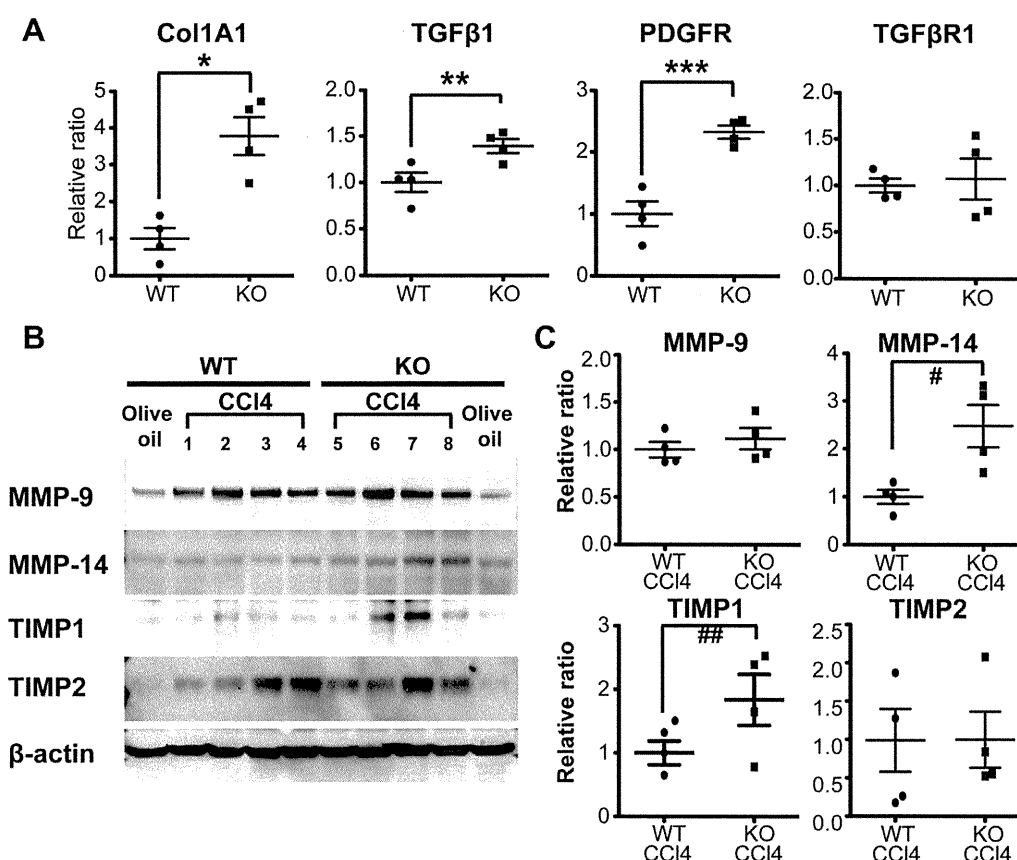


Fig. 2. Analysis of fibrosis-related molecules in the liver of CCl₄-treated MMP-2 KO and WT mice. (A) Relative expression of type I collagen (Col1A1), TGFβ1, PDGF receptor (PDGFR), and TGFβ receptor 1 (TGFβR1). Test samples were normalized to the copy number for β-actin, with equal copies applied as templates. Col1A1, TGFβ1, and PDGFR were significantly up-regulated in MMP-2 KO liver as compared with WT liver. **P* = 0.008. ***P* = 0.02. ****P* = 0.006. (B) Immunoblot assays of MMP-9, MMP-14, TIMP1, and TIMP2. (C) Quantitative analysis using densitometry. Production of MMP-14 and TIMP1 in the liver was increased in CCl₄-treated MMP-2 KO mice as compared with CCl₄-treated WT mice. #*P* = 0.01. ##*P* = 0.03. Values represent the ratio relative to the mean for CCl₄-treated WT mice. Bars represent means ± SEM. The result is representative of 3 independent experiments.

production of MMP-9 and TIMP2 in CCl₄-treated KO mice was almost equal to that in CCl₄-treated WT mice (Fig. 2C). These data indicated that molecules related to stellate cell activation and fibrosis were up-regulated in CCl₄-treated MMP-2 KO livers as compared with CCl₄-treated WT livers, suggesting that loss of MMP-2 promoted the activation of hepatic stellate cells during CCl₄-induced liver fibrosis.

3.4. Enhanced cholestatic fibrosis in MMP-2 KO mouse liver

Cholestatic fibrosis induced by BDL in MMP-2 KO and WT mice was analyzed at 2-weeks post-induction. Blood biochemical testing showed severe hyperbilirubinemia in mice treated with BDL (Table S2). The serum level of GGT was significantly higher in BDL-treated MMP-2 KO mice as compared with BDL-treated WT mice, whereas no significant change in T-Bil, AST, and ALT was found in either group (Table S2). Microscopic analysis of liver specimens showed extensive bile ductule proliferation and peribiliary fibrosis in BDL-treated mice (Fig. 3A). Bile ductule proliferation was more severe in BDL-treated MMP-2 KO mice than in BDL-treated WT mice (Fig. 3A). Sirius red staining analysis demonstrated more severe BDL-induced peribiliary fibrosis in KO mice than in WT mice (Fig. 3B). The fibrosis areas, quantified using an image analysis system, were significantly increased in BDL-treated KO mice as compared with BDL-treated WT mice (Fig. 3C). There was no difference in hepatic fibrosis area between WT and MMP-2 KO sham-operated mice (Fig. S2). This data indicated that

cholestatic-induced liver fibrosis was exacerbated in MMP-2 KO mice as compared with WT mice.

3.5. Hepatic αSMA production in MMP-2 KO mice with BDL-induced fibrosis

Hepatic αSMA production was assessed to determine changes in hepatic myofibroblasts associated with cholestatic-induced fibrosis. The size of αSMA-positive areas in the liver did not differ significantly between WT and MMP-2 KO sham-operated mice (Fig. S3A). Hepatic αSMA in BDL-treated mice was detected in periportal regions only. The αSMA-positive area in the liver of BDL-treated MMP-2 KO mice was almost equal to that of BDL-treated WT mice (Fig. S3A). As well as immunostaining analysis, immunoblot analysis showed that hepatic αSMA production in BDL-treated MMP-2 KO mice was almost equal to that in BDL-treated WT mice (Fig. 3D). Quantitative analyses using an image analysis system and densitometry also showed that hepatic αSMA production in BDL-treated MMP-2 KO mice was not significantly increased relative to WT mice (Figs. S3B and 3E).

3.6. Expression of fibrosis-related molecules in MMP-2 KO mice with cholestatic-induced fibrosis

The hepatic expression of molecules related to the promotion of liver fibrosis was studied in MMP-2 KO and WT mice with BDL-treated fibrosis. Quantitative RT-PCR analysis showed that hepatic

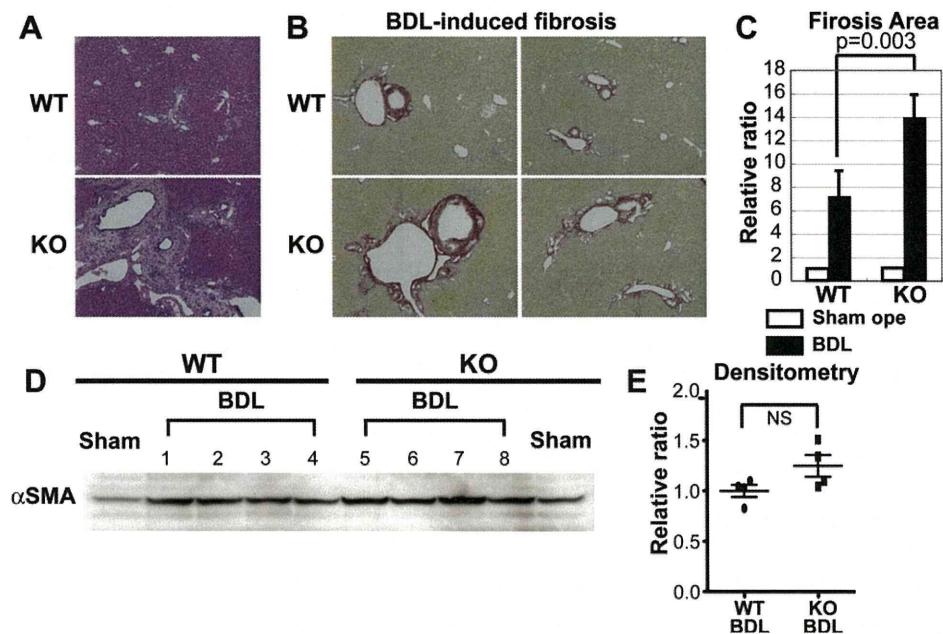


Fig. 3. Cholestasis-induced liver fibrosis is accelerated in MMP-2 KO mice. MMP-2 KO mice and WT littermates ($n = 4$ per group) were subjected to bile duct ligation (BDL). Negative control mice were sham operated (Sham). (A) Hematoxylin eosin staining of liver specimens of BDL-treated mice. (B) Representative photographs of Sirius red staining in the liver of BDL-treated mice. (C) Ratio of overall fibrosis area relative to sham-operated WT mice. Data represent means \pm SD. (D) Immunoblot analysis of α SMA in the liver of MMP-2 KO and WT mice. (E) Quantitative analysis of α SMA using densitometry. The α SMA protein in the immunoblot analysis was unchanged. Values represent the ratio relative to the mean for BDL-treated WT mice. Bars represent means \pm SEM.

expression of type I collagen, TIMP1, MMP-9, MMP-14, PDGF receptor, and TGF β was up-regulated in BDL-treated mice as compared with sham-operated mice (Figs. 4A and S4). Hepatic expression of type I collagen in BDL-treated KO mice was 2-fold higher than that in BDL-treated WT mice (Fig. 4A). The hepatic expression of TIMP1 was also up-regulated in BDL-treated KO mice (Fig. 4A). However, there was no significant difference in the hepatic expression of MMP-9, MMP-14, TGF β , TGF β receptor, or PDGF receptor between BDL-treated KO and BDL-treated WT mice (Figs. 4A and S4).

Immunoblot analysis showed that the levels of MMP-9, MMP-14, TIMP1 and TIMP2 protein in the liver were higher in BDL-treated mice as compared with sham-operated mice, indicating that production of fibrosis-related molecules was up-regulated in our experimental model (Fig. 4B). Quantitative analysis using densitometry showed that hepatic TIMP1 production was significantly higher in BDL-treated KO mice than BDL-treated WT mice (Fig. 4C). There was no significant difference in the production of MMP-9, MMP-14, or TIMP2 between BDL-treated KO mice and BDL-treated WT mice. Our data indicated that type I collagen and TIMP1 was up-regulated in BDL-treated MMP-2 KO mice as compared with WT mice, suggesting that TIMP1 production is related to acceleration of cholestasis-induced fibrosis in the liver of MMP-2 KO mice.

4. Discussion

In the present study, we analyzed liver fibrosis and fibrosis-related molecules in MMP-2 KO mice in models of toxin- and cholestasis-induced fibrosis. This is the first study to show that BDL-induced hepatic fibrosis is accelerated in MMP-2 KO mice, and that the expression of type I collagen is increased (Figs. 3C and 4A). BDL duplicates the hepatocytic damage, activation of hepatic stellate cells, and liver fibrosis observed in human liver disease. In the early phase of BDL, there is a marked and transient proliferation of bile duct epithelial cells associated with prolifera-

tion of portal periductular fibroblasts which rapidly express α SMA [16]. This supports the hypothesis that portal myofibroblasts play an important role in BDL-induced fibrogenesis. Myofibroblastic differentiation of portal fibroblasts is mediated by several signaling pathways including the TGF β [17] and PDGF [18] pathways. Our data indicate that these molecules were up-regulated in the liver of BDL-treated mice as compared with sham-operated mice, in consistent with previous reports. Hepatic α SMA production in MMP-2 KO mice was almost equal to that of WT mice (Fig. 3E), and the hepatic expression of TGF β 1, TGF β receptor, and PDGF receptor in BDL-treated MMP-2 KO liver was unchanged in comparison with BDL-treated WT liver (Figs. 4A and S4). Taken together, our data suggest that the myofibroblastic differentiation of portal fibroblasts in KO liver was almost equal to that of WT liver.

Hepatic TIMP1 was up-regulated in BDL-treated MMP-2 KO mice as compared with BDL-treated WT mice (Figs. 4A and 4C), indicating that loss of MMP-2 in cholestatic liver induces the TIMP1 production. In BDL-induced liver fibrosis, TIMP1 is expressed in myofibroblasts. However, loss of TIMP1 activity does not result in improvement of liver fibrosis as indicated by a previous study in TIMP1/TIMP2 double-KO mice, which showed that TIMP1 and TIMP2 do not play an essential role in experimental hepatic fibrogenesis by schistosomiasis [19]. The mechanism of TIMP1 up-regulation in MMP-2 KO liver remains unclear; however, it is possible that the ability of MMP-2-deficient portal fibroblasts to suppress TIMP1 production is impaired due to lack of MMP-2-mediated signaling. Further study is necessary to address this issue.

Previous studies have indicated that hepatic stellate cells undergo an activation process, acquire a fibroblastic phenotype, express α SMA, and play a major role in collagen deposition in CCl $_4$ -induced liver fibrosis [1,20]. TGF β induces the production of type I collagen in activated hepatic stellate cells. PDGF receptor is up-regulated in activated hepatic stellate cells proliferating in response to PDGF. Progression of CCl $_4$ -induced liver fibrosis is

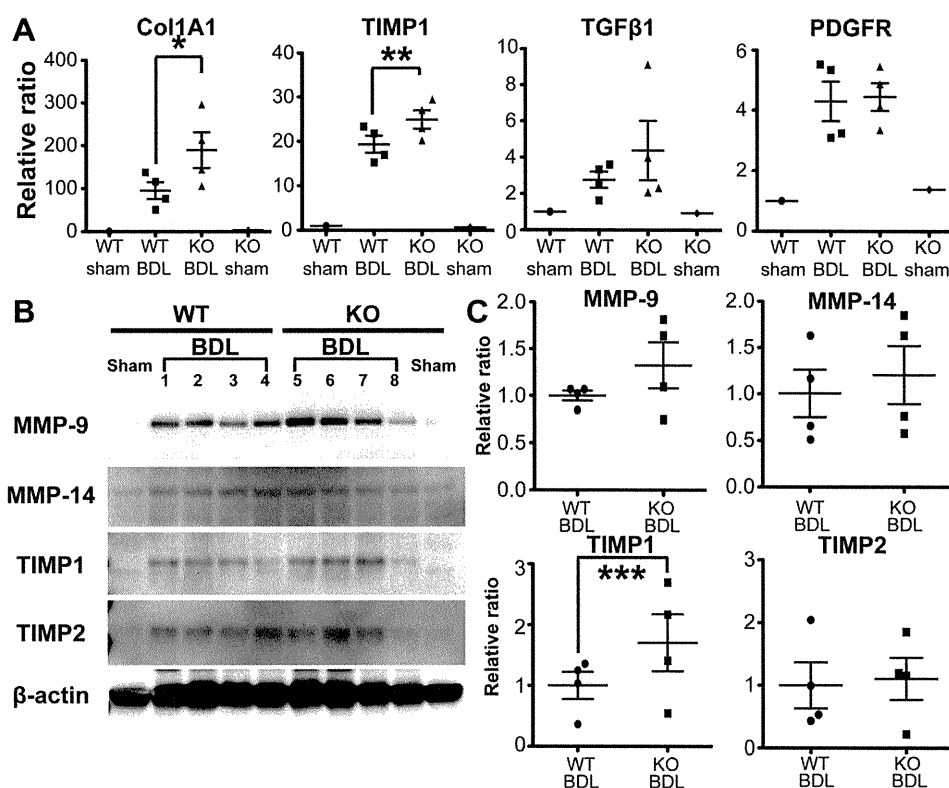


Fig. 4. Analysis of fibrosis-related molecules in the liver of BDL-treated mice. (A) Relative expression of Col1A1, TIMP1, TGFβ1, and PDGFR. Test samples were normalized to the copy number for β-actin, with equal copies applied as templates. Hepatic expression of Col1A1 and TIMP1 was significantly up-regulated in BDL-treated MMP-2 KO mice as compared with BDL-treated WT mice. Values represent the ratio relative to the mean for sham-operated WT mice. (B) Immunoblot assays of MMP-9, MMP-14, TIMP1, and TIMP2. (C) Quantitative analysis using densitometry. Hepatic production of TIMP1 in BDL-treated MMP-2 KO mice was increased as compared with BDL-treated WT mice. Values represent the ratio relative to the mean for BDL-treated WT mice. Bars represent means ± SEM. * $P = 0.02$. ** $P = 0.003$. *** $P = 0.04$. The result is representative of 3 independent experiments.

mediated by these molecules. Our data suggest that activation of hepatic stellate cells was promoted in MMP-2 KO mice as compared with WT mice. This is supported by the observation that the production of α SMA and TIMP1 was increased in MMP-2 KO liver (Figs. 1 and 2), because the activated hepatic stellate cells (myofibroblasts) are a major source of TIMP1 [21]. Thus, our data suggest the activation of hepatic stellate cells was promoted by loss of MMP-2 activity *in vivo*. Previous research has shown that loss of MMP-2 amplifies CCl₄-induced liver fibrosis, but no increase was seen in the *in vivo* levels of several molecules related to activation of hepatic stellate cells [22]. This discrepancy may be due to the duration of chronic CCl₄ administration, which was twice as long in our study. Increased hepatic levels of MMP-14 protein in CCl₄-treated MMP-2 KO mice may be due to a compensatory effect for MMP-2 deficiency, which is generally activated by MMP-14.

Classical substrates of MMPs are components of the ECM; however, the list of substrates has been extended to include various receptors, ligands and adhesion molecules [2]. Several studies have demonstrated changes in the hepatic fibrotic response in MMP-deficient mice. Madala et al. reported that chronic helminth-induced liver fibrosis was attenuated in MMP-12 deficient mice. MMP-12 deficiency is associated with up-regulation of ECM-degrading enzymes such as MMP-2, -9, and -13 in Th2 cytokine-driven fibrosis [23]. Furthermore, loss of ECM-degrading MMPs does not always lead to progression of liver fibrosis. MMP-13 is one of the representative ECM-degrading enzymes in mice. In the liver of BDL-treated MMP-13 KO mice, activation of hepatic stellate cells was paradoxically suppressed in comparison with WT mice [8], suggesting that MMP-13 probably contributes to accelerating fibrogenesis in cholestatic livers by mediating inflammation rather

than promoting fibrolysis. On the other hand, our data showed that MMP-2 contributes to suppression of fibrogenesis in both toxin- and cholestasis-induced liver damage. One possible interpretation is that MMP-2-mediated signaling is associated with the suppression of inflammation or fibrosis, which influence the production of type I collagen and TIMP1 derived from myofibroblasts. Another is that MMP-2 simply contributes to acceleration of fibrolysis. Radbill et al. showed that the expression of type I collagen in cultured hepatic stellate cells was decreased by knockdown of MMP-2 [22], suggesting that MMP-2-mediated signals directly regulate the expression of type I collagen. Thus, development of specific activators of MMP-2, but not of other ECM-degrading enzymes, could be promising as a new therapeutic strategy for the treatment of liver cirrhosis.

Acknowledgments

This work was supported in part by Grants-in-Aid for Scientific Research from the Ministry of Education, Culture, Sports, Science and Technology in Japan, the Ministry of Health, Labor and Welfare in Japan, the Japan Society for the Promotion of Science, Japan Health Sciences Foundation, National Institute of Biomedical Innovation, and the Foundation for Advancement of International Science. We thank Dr. S. Itohara for providing us MMP-2 deficient mice. We thank Prof. Y. Inagaki and Dr. T. Moro in Tokai University for helpful discussions about the method for bile duct ligation. We also thank Y. Wakiyama, K. Okada, K. Itoh, H. Itoh, and A. Yanagida in Division of Stem Cell Therapy, Institute of Medical Science, University of Tokyo for excellent technical assistance.

Appendix A. Supplementary data

Supplementary data associated with this article can be found, in the online version, at doi:10.1016/j.bbrc.2011.02.012.

References

- [1] S. Hemmann, J. Graf, M. Roderfeld, et al., Expression of MMPs and TIMPs in liver fibrosis – a systematic review with special emphasis on anti-fibrotic strategies, *J. Hepatol.* 46 (2007) 955–975.
- [2] M. Seiki, The cell surface: the stage for matrix metalloproteinase regulation of migration, *Curr. Opin. Cell Biol.* 14 (2002) 624–632.
- [3] S.L. Friedman, Evolving challenges in hepatic fibrosis, *Nat. Rev. Gastroenterol. Hepatol.* 7 (2010) 425–436.
- [4] R. Lichtinghagen, M.J. Bahr, M. Wehmeier, et al., Expression and coordinated regulation of matrix metalloproteinases in chronic hepatitis C and hepatitis C virus-induced liver cirrhosis, *Clin. Sci.* 105 (2003) 373–382.
- [5] T. Takahara, K. Furui, J. Funaki, et al., Increased expression of matrix metalloproteinase-II in experimental liver fibrosis in rats, *Hepatology* 21 (1995) 787–795.
- [6] A.E. Kossakowska, D.R. Edwards, S.S. Lee, et al., Altered balance between matrix metalloproteinases and their inhibitors in experimental biliary fibrosis, *Am. J. Pathol.* 153 (1998) 1895–1902.
- [7] T. Watanabe, M. Niioka, A. Ishikawa, et al., Dynamic change of cells expressing MMP-2 mRNA and MT1-MMP mRNA in the recovery from liver fibrosis in the rat, *J. Hepatol.* 35 (2001) 465–473.
- [8] H. Uchinami, E. Seki, D.A. Brenner, et al., Loss of MMP 13 attenuates murine hepatic injury and fibrosis during cholestasis, *Hepatology* 44 (2006) 420–429.
- [9] M. Seiki, N. Koshikawa, I. Yana, Role of pericellular proteolysis by membrane-type 1 matrix metalloproteinase in cancer invasion and angiogenesis, *Cancer Metastasis Rev.* 22 (2003) 129–143.
- [10] R. Issa, X. Zhou, C.M. Constandinou, et al., Spontaneous recovery from micronodular cirrhosis: evidence for incomplete resolution associated with matrix cross-linking, *Gastroenterology* 126 (2004) 1795–1808.
- [11] Y. Osawa, Y.A. Hannun, R.L. Proia, et al., Roles of AKT and sphingosine kinase in the antiapoptotic effects of bile duct ligation in mouse liver, *Hepatology* 42 (2005) 1320–1328.
- [12] T. Itoh, T. Ikeda, H. Gomi, et al., Unaltered secretion of beta-amyloid precursor protein in gelatinase A (matrix metalloproteinase 2)-deficient mice, *J. Biol. Chem.* 272 (1997) 22389–22392.
- [13] E.L. Opie, M.B. Rothbard, Osmotic homeostasis maintained by mammalian liver, kidney, and other tissues, *J. Exp. Med.* 97 (1953) 483–497.
- [14] S. Kakinuma, H. Ohta, A. Kamiya, et al., Analyses of cell surface molecules on hepatic stem/progenitor cells in mouse fetal liver, *J. Hepatol.* 51 (2009) 127–138.
- [15] S. Kakinuma, Y. Tanaka, R. Chinzei, et al., Human umbilical cord blood as a source of transplantable hepatic progenitor cells, *Stem Cells* 21 (2003) 217–227.
- [16] J.A. Dranoff, R.G. Wells, Portal fibroblasts: underappreciated mediators of biliary fibrosis, *Hepatology* 51 (2010) 1438–1444.
- [17] Z. Li, J.A. Dranoff, E.P. Chan, et al., Transforming growth factor-beta and substrate stiffness regulate portal fibroblast activation in culture, *Hepatology* 46 (2007) 1246–1256.
- [18] N. Kinnman, C. Francoz, V. Barbu, et al., The myofibroblastic conversion of peribiliary fibrogenic cells distinct from hepatic stellate cells is stimulated by platelet-derived growth factor during liver fibrogenesis, *Lab. Invest.* 83 (2003) 163–173.
- [19] B. Vaillant, M.G. Chiaramonte, A.W. Cheever, et al., Regulation of hepatic fibrosis and extracellular matrix genes by the response: new insight into the role of tissue inhibitors of matrix metalloproteinases, *J. Immunol.* 167 (2001) 7017–7026.
- [20] K. Wake, "Sternzellen" in the liver: perisinusoidal cells with special reference to storage of vitamin A, *Am. J. Anat.* 132 (1971) 429–462.
- [21] E. Roeb, E. Purucker, B. Breuer, et al., TIMP expression in toxic and cholestatic liver injury in rat, *J. Hepatol.* 27 (1997) 535–544.
- [22] B.D. Radbill, R. Gupta, M.C. Ramirez, et al., Loss of matrix metalloproteinase-2 amplifies murine toxin-induced liver fibrosis by upregulating collagen I expression, *Dig. Dis. Sci.* 56 (2011) 406–416.
- [23] S.K. Madala, J.T. Pesce, T.R. Ramalingam, et al., Matrix metalloproteinase 12-deficiency augments extracellular matrix degrading metalloproteinases and attenuates IL-13-dependent fibrosis, *J. Immunol.* 184 (2010) 3955–3963.

Original Article

Studies on virus kinetics using infectious fluorescence-tagged hepatitis C virus cell culture

Machi Yamamoto,^{1*} Naoya Sakamoto,^{1,2*} Tetsuya Nakamura,^{1,3} Yasuhiro Itsui,^{1,5} Mina Nakagawa,^{1,2} Yuki Nishimura-Sakurai,¹ Sei Kakinuma,^{1,2} Seishin Azuma,¹ Kiichiro Tsuchiya,¹ Takanobu Kato,⁴ Takaji Wakita⁴ and Mamoru Watanabe¹

¹Department of Gastroenterology and Hepatology, ²Department for Hepatitis Control, ³Department of Advanced Therapeutics in Gastrointestinal Diseases, Tokyo Medical and Dental University, ⁴Department of Virology II, National Institute of Infectious Disease, Tokyo, and ⁵Department of Internal Medicine, Soka Municipal Hospital, Saitama, Japan

Aim: Studies of the complete hepatitis C virus (HCV) life cycle have become possible with the development of a HCV-JFH1 cell culture system.

Methods: In this study, we constructed two fluorescence protein-tagged recombinant JFH1 virus clones, JFH1-EYFP and JFH1-AsRed, as well as two corresponding clones with adaptive mutations, JFH1-EYFP mutant and JFH1-AsRed mutant, that and were as effective as JFH1 in producing infectious virus particles, and investigated their viral infection life cycles.

Results: After infection of the fluorescence-tagged mutant viruses, infected cells increased exponentially. In cells, EYFP or AsRed and NS5A were expressed as a fusion protein and

co-localized in core proteins. The rate of the cell–cell spread was dependent on the cell densities with a maximum of $10^{2.5}$ /day. Treatment of cells with interferon or a protease inhibitor suppressed expansion of virus-positive cells.

Conclusion: Taken together, these results indicate that fluorescence-tagged HCV is a useful tool to study virus infection life cycles and to assist in the search for novel antiviral compounds.

Key words: AsRed, confocal laser microscopy, HCV-JFH1 cell culture, protease inhibitor, yellow fluorescence protein

INTRODUCTION

HEPATITIS C VIRUS (HCV) infection is characterized frequently by chronic inflammation of the liver, leading to decompensated liver cirrhosis and hepatocellular cancers.¹ Interferon (IFN)- α has been the mainstay of HCV therapy.² However, the most effective therapy, pegylated IFN plus ribavirin in combination, can eliminate HCV from only half of the patients treated^{3,4} and often is accompanied by substantial side-effects.^{5,6} These difficulties in eliminating the virus are attributable mostly to the limited treatment options.⁷

Hepatitis C virus belongs to the family Flaviviridae. The viruses have positive-strand RNA genomes of approximately 10 kb that encode polyproteins of approximately 3000 amino acids. The protein is post-translationally processed by cellular and viral proteases into at least 10 mature proteins. The viral non-structural (NS) proteins accumulate in the endoplasmic reticulum (ER) and they direct genomic replication and viral protein synthesis.^{8,9} Studies of the HCV life cycle and the development of new drugs have long been hampered by the lack of cell culture systems. These problems have been greatly overcome by the development of the HCV subgenomic replicon¹⁰ and HCV-JFH1 cell culture¹¹ systems.

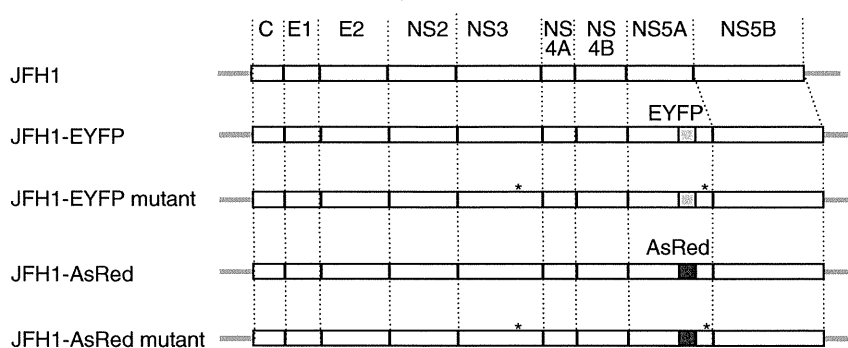
After the development of HCV-JFH1 cell culture, many variations of reporter protein-tagged HCV systems have been described.^{12–15} These reporter systems, however, feature poor or absent virus propagation, secretion and re-infection. The C-terminal end of the NS5A region, which has been used for insertion of

Correspondence: Dr Naoya Sakamoto, Department of Gastroenterology and Hepatology, Tokyo Medical and Dental University, 1-5-45 Yushima, Bunkyo-ku, Tokyo 113-8519, Japan. Email: nsakamoto.gast@tmd.ac.jp

*M. Y. and N. S. contributed equally to this work.

Received 15 July 2010; revised 21 November 2010; accepted 12 December 2010.

Figure 1 Schematic of the JFH1-based hepatitis C virus constructs. EYFP or AsRed was inserted in-frame into the *CpoI* site of NS5A (JFH1-EYFP or JFH1-AsRed). The adaptive mutations in NS3 and NS5A (T4209A and C7653T) are indicated by asterisks (JFH1-EYFP mutant or JFH1-AsRed mutant).



reporter sequences, does not affect viral genomic replication,¹² while manipulation of the domain resulted in the loss of viral particle secretion possibly through abrogation of NS5A-core protein–protein association that is crucial for the viral particle assembly.¹⁶ These problems have made it difficult to analyze the entire viral life cycle in living cells. Recently, Han *et al.* reported a mutant HCV-JFH1 clone that expressed green fluorescent protein (GFP)-tagged NS5A and which could propagate and secrete infectious virus particles.¹⁷

In this study, we took advantage of the mutant fluorescence protein-tagged HCV and investigated the life cycles of HCV infection. We have demonstrated the rate of expansion of HCV infection using flow cytometry. Moreover, we have shown the kinetics of co-infection with two virus strains, which differed in their ability to secrete infectious virus particles.

METHODS

Reagents

RECOMBINANT HUMAN IFN- α -2b was from Schering-Plough (Kenilworth, NJ). Protease inhibitor (BILN2061) was from Boehringer Ingelheim (Ingelheim, Germany). BILN2061 is a macrocyclic NS3 protease inhibitor, the antiviral effects of which have been reported in a phase I clinical study.¹⁸ Although further development of BILN2061 has been abandoned, this compound has structural homology with other protease inhibitors that are currently being evaluated in clinical trials, such as TMC435 and MK7009.^{7,19}

Cell culture

Huh7.5.1 cells²⁰ and their derivatives were maintained in Dulbecco's modified minimal essential medium

(DMEM; Sigma, St Louis, MO, USA) with 10% fetal bovine serum (FBS; Invitrogen, San Diego, CA, USA) at 37°C under 5% CO₂.

Plasmid constructs (Fig. 1)

In order to produce pJFH1-EYFP, the EYFP gene was amplified from pEYFP-C1 (Clontech, Mountain View, CA, USA) by polymerase chain reaction (PCR). The PCR products were then inserted into the *CpoI* site (7484) of pJFH1. Similarly, pJFH1-AsRed was produced using pAsRed2 (Clontech). The JFH1-EYFP and JFH1-AsRed mutants, which are JFH1-based mutants with robust virus production capability, have two point mutations (T4209A, C7653T).¹⁷ In order to introduce these mutations into pJFH1-AsRed, the *AvrII/NsiI* and *BsrGI* fragments of pJFH1-AsRed were amplified by PCR. The PCR products were subcloned into the T-Vector (pGEM-T Easy Vector Systems; Promega, Madison, WI, USA) and the mutations were introduced by site-directed mutagenesis (Quick-Change II Site-Directed Mutagenesis Kit; Stratagene, La Jolla, CA, USA), as reported previously.²¹ Finally, these *AvrII/NsiI* and *BsrGI* fragments were reinserted into the parental plasmid, pJFH1-AsRed. The pJFH1-AsRed mutant was digested with *CpoI* and the DNA fragment was subcloned into pJFH1-EYFP, producing the mutant pJFH1-EYFP. All nucleotide numbers refer to pJFH1.¹¹

Constitutive expression of ER-fluorescence protein in Huh7.5.1 cells

Huh7.5.1 cells were seeded into 6-cm diameter dishes and transfected with pDsRed2-ER (Invitrogen) using Lipofectamine 2000 (Invitrogen) according to the manufacturer's protocol. Isolated clones (ER-Huh7.5.1 cells) were maintained under selection with 0.75 mg/mL G418 (Nacalai Tesque, Kyoto, Japan) and

screened for DsRed protein expression using fluorescence microscopy (BZ-8000; Keyence, Tokyo, Japan).

RNA transcription and transfection

Recombinant HCV RNA was synthesized and transfected as previously described.^{22,23} Briefly, the plasmids were linearized by digestion with *Xba*I and subjected to *in vitro* transcription using RiboMax Large Scale RNA Production System (Promega). For the RNA transfection, Huh7.5.1 cells were suspended in Opti-MEM (Invitrogen) containing 10 µg of HCV RNA, transferred into a 4-mm electroporation cuvette, and subjected to an electric pulse (1050 µF and 270 V) using the Gene Pulser II apparatus (Bio-Rad, Richmond, CA, USA). After electroporation, the cell suspension was left for 5 min at room temperature and then incubated under normal culture conditions in a 10-cm diameter dish. The transfected cells were split every 3–5 days. The culture media were transferred subsequently onto uninfected Huh7.5.1 cells.

Immunofluorescence microscopy

Immunofluorescence microscopy was performed as described previously.²⁴ Cells were cultured on 18-mm round cover slips (Matsunami, Osaka, Japan) and fixed using 4% paraformaldehyde for 10 min at room temperature. Cells were incubated with the primary antibodies for 1 h at 37°C and with Alexa Fluor 488 goat antimouse immunoglobulin (Ig)G antibody (Molecular Probes, Eugene, OR, USA) for 1 h at room temperature in the dark. Mouse anti-NS5A antibody (Biodesign, Saco, ME, USA) and mouse anti-core antibody (Abcam, Cambridge, MA, USA) were used as primary antibodies. Cells were mounted with VECTA SHIELD Mounting Medium with DAPI (Vector Laboratories, Burlingame, CA, USA) and visualized by confocal laser fluorescent microscopy (BZ-8000 [Keyence] and FLUOVIEW FV10i [Olympus, Tokyo, USA]).²⁵

Flow cytometry

JFH1-EYFP and JFH1-EYFP mutant-transfected Huh7.5.1 cells and uninfected Huh7.5.1 cells were cul-

tured in 12-well plates (Becton Dickinson, Franklin Lakes, NJ, USA). The cells were collected on the days, post-transfection or post-infection, indicated. After washing with phosphate buffered saline (PBS; Nacalai Tesque) supplemented with 3% FBS and staining of dead cells with propidium iodide, the cells were analyzed using a FACS Calibur with CellQuest software (Becton Dickinson).

Quantification of HCV core antigen in the culture medium

The culture media from Huh7.5.1 cells transfected with JFH1 and its derivatives were collected on the days indicated and stored at 80°C. The levels of core antigen in the culture media were measured using a chemiluminescence enzyme immunoassay (CLEIA) according to the manufacturer's protocol (Lumipulse Ortho HCV Antigen; Ortho-Clinical Diagnostics).

Western blotting

Western blotting was carried out as described previously.²¹ Briefly, 10 µg of total cell lysate was separated by sodium dodecylsulfate polyacrylamide gel electrophoresis and blotted onto a polyvinylidene fluoride membrane. The membrane was incubated with primary antibodies followed by peroxidase-labeled anti-IgG antibody and visualized by chemiluminescence using the ECL Western blotting Analysis System (Amersham Biosciences). The antibodies used were anti-core mouse monoclonal antibody 2H9, anti-NS5A mouse monoclonal antibody 9E10 (provided by Dr Rice), and anti-GFP rabbit polyclonal antibody (Invitrogen). The anti-GFP is able to detect EYFP. To confirm expression of EGFP in Huh 7.5.1 cells, Huh7.5.1 cells were seeded into a 6-cm diameter dish and transfected with pEGFP (Invitrogen) using Lipofectamine 2000 (Invitrogen).

Statistical analyses

Statistical analyses were performed using Welch's *t*-test. *P*-values of less than 0.05 were considered statistically significant.

Figure 2 Infectious hepatitis C virus (HCV) reporter virus with robust virus production capability. (a) Huh7.5.1 cells were transfected with JFH1-EYFP, JFH1-EYFP mutant, JFH1-AsRed or JFH1-AsRed mutant HCV RNA. At 3 days post-transfection, culture media were collected and added onto uninfected cells. At the days indicated, EYFP or AsRed-directed-fluorescence was visualized directly. (b) The ratio of EYFP or AsRed-positive cells in (a) is counted in each image and plotted vs time. Assays were carried out in triplicate and the results are expressed as mean ± standard deviation. **P* < 0.05. —●—, JFH1-EYFP mutant; -○-, JFH1-EYFP; —▲—, JFH1-AsRed mutant; -☆-, JFH1-AsRed. (c) The levels of core antigen in the culture medium of JFH1, JFH1-EYFP, JFH1-EYFP mutant, JFH1-AsRed, and JFH1-AsRed mutant-transfected Huh7.5.1 cells collected on the days indicated. Ag, antigen. -■-, JFH1; -○-, JFH1-EYFP; —●—, JFH1-EYFP mutant; -☆-, JFH1-AsRed; —▲—, JFH1-AsRed mutant.

